



RILEM TC 277-LHS report: a review on the mechanisms of setting and hardening of lime-based binding systems

J. I. Alvarez · R. Veiga · S. Martínez-Ramírez · M. Secco ·
P. Faria · P. N. Maravelaki · M. Ramesh · I. Papayianni ·
J. Válek

Received: 29 October 2020 / Accepted: 7 February 2021 / Published online: 5 March 2021
© The Author(s) 2021, corrected publication 2022

Abstract The main objective of RILEM TC LHS-277 “Specifications for testing and evaluation of lime-based repair materials for historic Structures” is the revision, adaption and, when necessary proposal, of the test methods to accurately study lime-based binding systems and mixtures, such as mortars and grouts. The empiric use of the lime-based composites and the predominant employ of cement in the field of

Civil Engineering have led to the widespread application of test methods developed for cement-based composites to test the former. However, the clear differences in composition and performance between modern cement binders and lime-based materials would advise to explore specific test methods for the latter. To undertake this task the previous knowledge on the mechanisms of setting and hardening of these binders must be revised, arranged and synthesized. Processes such as drying, carbonation, hydration and pozzolanic reaction may occur during the setting and hardening of lime-based mortars and competition between them cannot be underestimated. With the aim of underpinning the revision and proposal of test methods for lime-based systems, this review paper reports a comprehensive study of the mechanisms of setting and hardening of these binders, considering the variability of the composition, which includes pure air lime as well as lime with hydraulic properties, lime-cement and lime-pozzolan systems.

Keywords Lime · Hydraulic · Carbonation · Drying · Pozzolanic reaction · Hydration

This review was prepared by José I. Alvarez, Rosário Veiga, Sagrario Martínez-Ramírez, Michele Secco, Paulina Faria, Pagona-Noni Maravelaki, Meera Ramesh, Ioanna Papayianni and Jan Válek within RILEM TC LHS-277 “Specifications for testing and evaluation of lime-based repair materials for historic Structures” and further reviewed and approved by all members of the RILEM TC LHS-277. TC Chair: Ioanna Papayianni. TC Deputy Chair: Jan Válek. Members: José I. Alvarez, Beril Bicer-Simsir, Violeta Bokan-Bosiljkov, Claudia Brito De Carvalho Bello, Arnaldo Manoel Carneiro, Paulina Faria, Liberato Ferrara, Caspar J.W.P. Groot, Davide Gulotta, Hande Gunozu Ulusoy, John J. Hughes, Ioannis Ioannou, Heejeong Kim, Loucas Kyriakou, Cristiana Lara Nunes, Pagona Maravelaki, Sagrario Martinez-Ramirez, Vasiliki Pachta, Andreja Padovnik, Ioanna Papayianni, Chiara Pasian, Giovanni Pesce, Ulrike Peter, Meera Ramesh, Divya Rani, Sara Pavia, Sriram Pradeep Saridhe, Michele Secco, Maria Stefanidou, Cristina Tedeschi, Magdalini Theodoridou, Lucia Toniolo, Jan Válek, Rob Van Hees, Maria Rosario Veiga.

J. I. Alvarez (✉)
Materials and Cultural Heritage, MATCH, Research Group, Department of Chemistry, School of Sciences, University of Navarra, C/Irunlarrea, 1, 31008 Pamplona, Navarra, Spain
e-mail: jalvarez@unav.es

R. Veiga
Buildings Department, National Laboratory for Civil Engineering – LNEC, Av. do Brasil 101, 1700-066 Lisbon, Portugal
e-mail: rveiga@lnec.pt



1 Introduction

Despite the wide research on cement-based systems, the knowledge about the lime-bearing mixtures has been rather empiric. Nevertheless, these systems are continuously attracting interest, particularly for using them as repair materials for Built Heritage [1–8]. In addition, the employment of lime-based binders has positive environmental implications, due to their lower energy consumption and their lower contributions of the ingredients and processes to the global warming potential as compared with cement [9]. Their atmospheric CO₂ uptake properties are also useful to minimize the carbon dioxide footprint [10, 11].

Lime-based binding materials can be used in a wide variety of mixtures depending on their function [12], such as masonry bedding mortars [2, 13], renders and plasters [14–16], repointing materials as grouts [17–21], whitewash [22, 23], ornamental pieces [24], wall painting support [25, 26], finishing mortars [27], surface repair [28] or flooring mortars [29, 30]. All these materials can be produced from diverse raw materials, obtaining both air lime (calcitic [31, 32] and/or dolomitic [33–36]) or limes with hydraulic properties [37–39], all classified by EN 459-1 (2015) [40]. Furthermore, they can be blended with pozzolans [41–45] and cement [46–51]. The use in both new Civil Engineering applications and conservation of Architectural Heritage [52] demand all these types of materials. The quality of these composites and their

performance must be controlled and, in most cases, the procedures are based on cement analogues [53, 54]. However, modern calcium silicate cement-based binders display remarkable differences in terms of chemical and mineralogical composition and performance [50], and the assumptions for test and procedures lead to wrong results when directly applied to lime-based binders [55]. The technical committee RILEM TC LHS-277 “Specifications for testing and evaluation of lime-based repair materials for historic Structures” is focused on the revision, adaption and, when necessary proposal, of test methods to accurately study lime-based systems. Lime-bearing materials exhibit a slower setting and hardening than that of the cement ones [56]. Their water demand is also different [57–59], leading to different requirements for the preparation of the composites. Their mechanical strengths, modulus of elasticity and pore structure are quite distinct from those of cement composites [60–63]. And finally, their expected durability in different environments presents special features [64–69].

To ascertain the most suitable test methods for these lime-based binders, it is of utmost importance to bear in mind the different mechanisms of setting and hardening involved in these systems. These mechanisms differ from those taking place in cement materials and must be revised considering the diverse composition of the raw materials (consisting of aerial

S. Martínez-Ramírez
Instituto de Estructura de la Materia (IEM-CSIC),
C/Serrano 121, 28006 Madrid, Spain
e-mail: sagrario@iem.cfmac.csic.es

M. Secco
Department of Cultural Heritage (DBC), University of
Padova, Padova, Italy
e-mail: michele.secco@unipd.it

P. Faria
CERIS and Department of Civil Engineering,
Universidade NOVA de Lisboa, 2829-516 Caparica,
Portugal
e-mail: paulina.faria@fct.unl.pt

P. N. Maravelaki
School of Architecture, Technical University of Crete,
73100 Akrotiri, Chania, Greece
e-mail: nmaravel@elci.tuc.gr

M. Ramesh
Department of Civil Engineering, ISISE, Universidade Do
Minho, Guimaraes, Portugal
e-mail: rmeera.93@gmail.com

I. Papayianni
Laboratory of Building Materials, Department of Civil
Engineering, Aristotle University of Thessaloniki,
Thessaloniki, Greece
e-mail: papayian@civil.auth.gr

J. Válek
Institute of Theoretical and Applied Mechanics, Czech
Academy of Sciences, Prosecká, 809/76, 190 00 Prague 9,
Czech Republic
e-mail: valek@itam.cas.cz



and hydraulic components) and their possible blends. This TC report is one of the expected outputs of the activities of the RILEM TC LHS-277 and deals with the analysis of the mechanisms of setting and hardening of composites produced with lime-based binders. This document describes these mechanisms according to a comprehensive literature review, for pure air lime-systems, systems with limes with hydraulic properties (natural hydraulic lime or air lime with pozzolans), and lime-cement systems. The members of the RILEM TC LHS-277 agreed in the upper limit of 30% by mass of cement of the total binding system as composites to be studied, considering that mixtures with higher percentages will perform according to effects of the predominant cement phase.

This TC report is structured in five main sections, as follows. The first four sections focus on the main setting and hardening mechanisms, individually considered, for lime-bearing systems: drying, carbonation, hydration and pozzolanic reaction, being the two first sections of particular interest for pure air lime binders and the others for natural hydraulic lime, lime-cement and lime with pozzolan systems. The influence of the different factors has been discussed. These sections provide a significant basis to understand the relevant processes and factors that take place during the setting and stiffening of lime-bearing composites.

The last section tackles the competition between these individual mechanisms, providing response to important questions such as how the drying interferes with the carbonation or which relative humidity and temperature conditions enhance hydration instead of carbonation for a binder with hydraulic properties. The paper also includes discussions on the main aforementioned mechanisms (drying, carbonation, hydration and pozzolanic reaction) prevailing in the main types of binders: pure air lime (both calcitic and dolomitic lime), natural hydraulic lime, pozzolan-lime and lime-cement binders.

2 Drying of fresh mortars

Drying of fresh mortars is a critical stage during hardening of mortars and it has a significant influence on the microstructure and the performance of hardened mortars. Although the aggregate also influences

the drying, according to the objectives of this review, this section focuses on the binder-related factors.

Two different mechanisms are involved: (1) water consumption by hydraulic reactions (only in mortars with a hydraulic phase); (2) removal of water by evaporation and absorption by the substrate (for mortars in contact with porous media, which is the most frequent case on site).

2.1 Influence of different factors

Higher mixing water content means in general higher porosity [70], increased shrinkage and, in some cases (depending on the binder), mechanical characteristics decrease. According to Arizzi et al. [32], mortars with higher water content undergo higher drying shrinkage in the first few hours.

In binders with hydraulic phases or pozzolans, high content of mixing water may be favourable considering that it favours hydraulic reaction instead of carbonation [71, 72], although even in these binding systems the high water/binder ratio increases the porosity and decreases the strength [73]. However, for pure air lime systems, high ratio of water/binder retards carbonation and increases porosity, as well as the size of the pores [74].

Curing conditions, particularly temperature and relative humidity (RH), influence the kinetics of the hardening reactions, drying, hydration and carbonation, and subsequently mechanical strength and shrinkage. Lime mortars achieve higher strength when cured at moderate humidity conditions, for example at RH of $70 \pm 5\%$ during the first 28 days. Nevertheless, at high RH conditions, the carbonation is hindered, because the transport of CO_2 might be blocked [60]. In the case of nanolimes, when $\text{RH} > 70\%$ the formation of a multilayer water adsorption on $\text{Ca}(\text{OH})_2$ particles increases carbonation rate [75]. However if the RH is lower than 30% the dissolution of CO_2 is hindered.

Using specific test methods, it was verified [76] that the best curing conditions for hydraulic renders consist of periodic water spraying. Also, absorbent substrates seem to be favourable, but they must be humidified for better results. In hydraulic lime-mortars, like in cement-based mortars [77], internal moisture changes are ascribed to autogenous shrinkage during hydration of the hydraulic compounds (more intense in low water/binder ratio mixtures, < 0.40), and to external

Table 1 Summary of the factors influencing the optimal conditions for the carbonation of lime-based mortars

Factors affecting the carbonation rate in lime mortars	Conditions to enhance the carbonation rate
Relative humidity	In connection with the inner amount of water (mixing water ratio) Values of 40–80% [93] ($70 \pm 5\%$ according to [3])
CO ₂ partial pressure	Normal conditions Forced carbonation increases the speed although the heat release and the subsequent water evaporation should be considered [103, 105]
Filler ratio	Increasing values slow down the carbonation [104]
Masonry thickness	Permeability of the system [97, 100] to allow the proper CO ₂ diffusion
Small portlandite particle size	Related to the burning of the limestone (recommended between 850 and 900 °C) and to the slaking process (lime maturation) [110–113]

evaporation, which achieves removal of water from the matrix pore structure and causes significant volumetric shrinkage of the material (drying shrinkage), due to different kinds of stresses generated by the moisture gradients, which are well described by Scherer [78]: (a) Capillary pressure, which is the pressure in the capillary pores resulting from the interactions of forces of the liquid and vapour phases with the solid walls of the pores. The liquid flows from the interior to cover the solid structure interface, causing tensile stresses in the liquid and compression on the solid network; (b) Osmotic pressure, which is produced by a concentration gradient in solutions divided by a semipermeable membrane. In this case, the liquid inside the pores diffuses through their walls to reduce the salt concentration gradient produced by the evaporation near the drying surface. If the pores are small enough to delay the liquid transport, a tension is produced in the liquid, which is compensated by a compressive force in the solid network, producing shrinkage; (c) Disjoining pressure, which consists in repulsive forces, mainly of electrostatic origin, between solid layers and are enhanced by the liquid evaporation that tends to approximate the solid elements. The liquid transport is then promoted, by flow or diffusion, to depart the solid layers. These forces are more likely to be important near the end of the drying, when the solid layers are closer.

The several types of forces that promote the water transport may be analysed as a whole, using the concept of moisture potential, which, if the pore structure is assimilated to columns of water, would tend to produce an equilibrium height. The transport movements are different depending on the types of

forces: capillary pressure gradients produce flow, while concentration gradients (that produce osmotic pressure) cause diffusion.

In the case of pure air lime mortars, no hydraulic reactions are involved, thus the drying is achieved by water evaporation and, also in many cases, through water absorption by the substrate, which concerns all kinds of mortars in contact with porous media (such as plasters, renders, repointing, and bedding mortars). The stresses involved are the same described above, with predominance of capillary forces, as porosity is usually more concentrated in the capillary range.

Concerning the evaporation mechanism, in the first stage of drying the pores are full of liquid and there is a constant rate of liquid transport to the surface. Most of the shrinkage occurs in this phase and the drying stresses achieve a maximum, producing the highest drying shrinkage and greatest risk of cracking. The analysis of the stresses distribution in the liquid inside the pores network was found by Scherer [78] to be greatest near the drying surface. This stress variation produces differential shrinkage of the material and local tensile stresses, which can result in cracking. According to Scherer [78], the probability of fracture is related to: the size of the body, which in the case of a mortar is the thickness of the coat; the rate of evaporation, which is governed by external conditions, namely temperature, relative humidity and wind velocity; and the mechanical characteristics of the material network, namely the deformation under compressive forces.

In the second stage of drying, also called Falling Rate Period [78], the drying front recedes into the material and part of the pores stop being saturated.



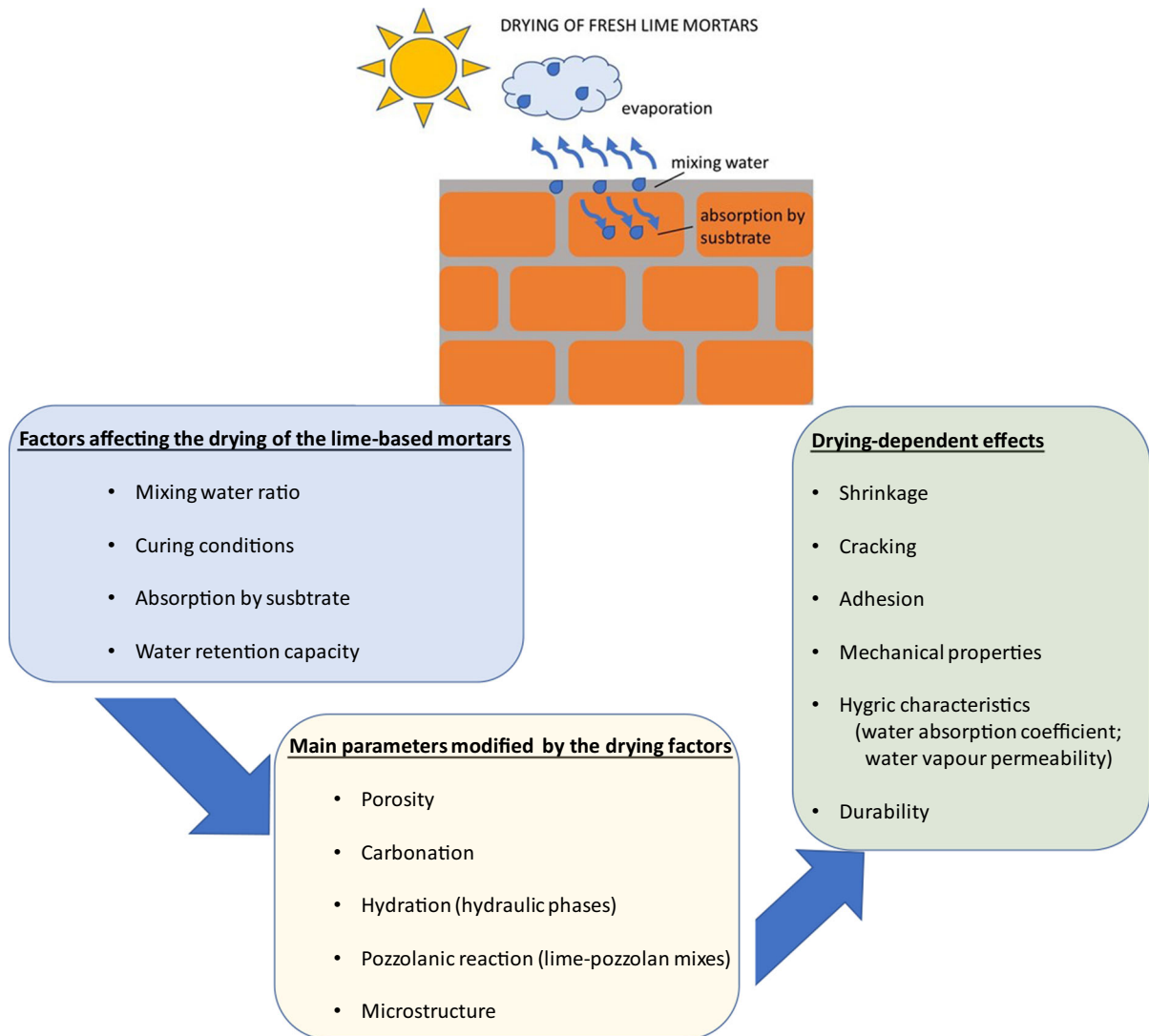


Fig. 1 Summary of the factors affecting the drying, the modified parameters and the consequences in the mortars dependent on the drying in lime-based binders

Then the water transport occurs in both liquid (in the saturated pores) and vapour state, by diffusion (in the pores where the liquid film becomes discontinuous). At this stage the water transport is determined by the properties of the material, especially by the pore sizes and interconnection among the pores [32, 78]. There is some expansion of the saturated region of the material, which partially compensates shrinkage, but some differential strains occur between the saturated and the non-saturated regions, which may cause cracks near the non-drying surface [78].

As for the water absorption by the substrate, the suction pressure depends on the relative size of pores of

mortar and substrate: small pores of the substrate exercise a suction pressure inducing the water transport from the larger pores of the mortar. This mechanism is particularly significant for air lime mortars. In fact, those mortars have a higher volume of large pores [79] and so a higher percentage of the substrate pores will be smaller than those of mortars and will be able to apply suction pressure. The influence of substrate absorption in these mortars concerns drying and microstructural changes, such as porosity [70, 80, 81]. In all cases, both external evaporation and substrate suction promote microstructural modification together with possible cracking [71, 76].

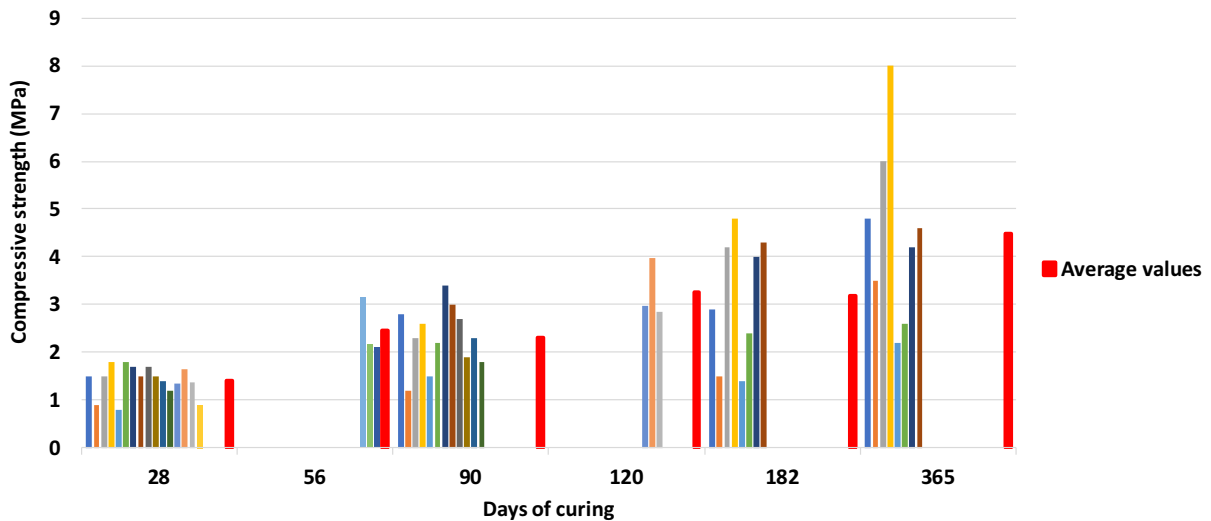


Fig. 2 Compressive strength values of different datasets of dolomitic lime mortars vs curing time

The absorption of water by the substrate causes a reduction of water in the mortar, leading to a decrease in its open porosity [70]. The higher the water absorption of the substrate, the greater the influence on its open porosity and bulk density [82]. Generally, a more significant reduction of open porosity occurs for a more porous substrate. A good correlation was observed between open porosity and bulk density (inverse relation) and between these two characteristics and open porosity of the substrate [70, 76].

If the water absorption of the substrate is too high, it may desiccate the mortar, which is unfavourable especially for hydraulic binders, as it may hinder hydraulic reactions. The humidification of the substrate previously to mortar application should be carried out to prevent this effect. As shown by several studies [77, 83, 84], more severe drying conditions, namely with higher drying rates and higher temperature, result in more intense cracking. Even when the macroscopic shrinkage does not significantly increase, at the microscopic level there are differential strains that origin micro-cracking. In these more severe conditions, both the effect of hindering the hydration of the hydraulic binders and the production of microcracks, reflect in the microstructure in the opposite sense, resulting in a coarser pore structure [77, 83], thus increasing the porosity, instead of reducing it.

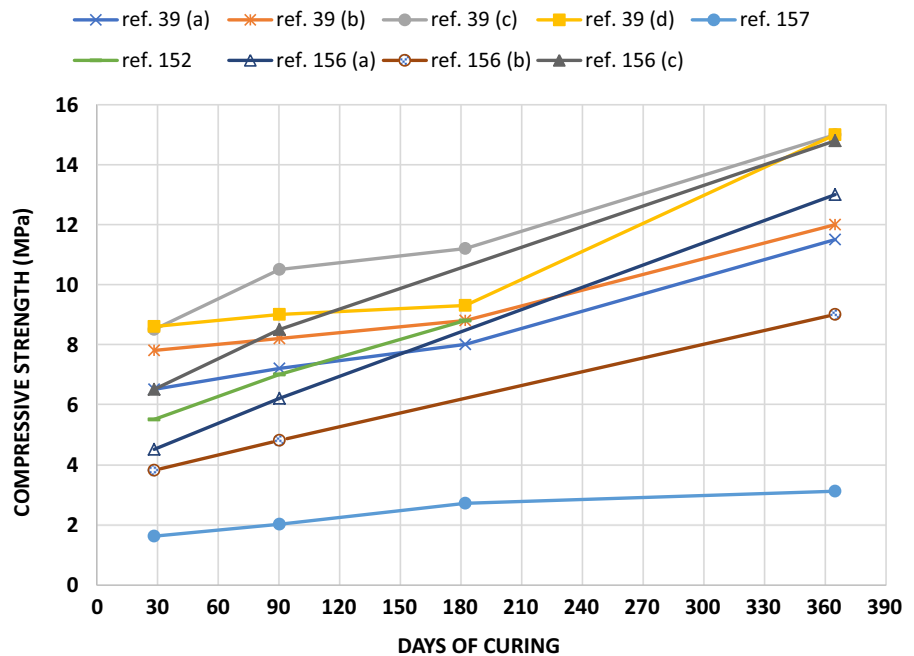
Water retention capacity of mortars has an influence on drying. More water retentiveness leads to

lower drying rates, both by evaporation and by suction of the substrate. This effect naturally promotes better hydration, in the case of lime binders with a hydraulic phase and may also produce good conditions for carbonation, assuring enough moisture content, however moderate, during a long period, even in dry external conditions. Figure 1 depicts the main factors influencing drying.

2.2 Effects on the agglomeration and crystalline structure of the binder particles

Drying promotes a general compression of the solid structure that arises as a reaction to the tensile state of the liquid phase caused by the flow of liquid to the exterior. In particular for hydraulic binders, this compression state results in increased bonding between C–S–H particles [32]. In air lime-mortars drying conditions, namely RH and drying rate influence the crystallization mode. For example, according to López-Arce et al. [85], carbonation of nanolime at RH between 75 and 90% gives rise to amorphous and crystalline calcium carbonate (calcite, aragonite and vaterite). However, at low RH (33–54%) only crystalline calcium carbonate as vaterite is formed. Under room conditions, the carbonation process of the nanolime is as follows: initially, the amorphous calcium carbonate (ACC) is formed, through a dissolution–precipitation or homogeneous nucleation process. Then, and after the ACC dissolution, the

Fig. 3 Compressive strength versus curing times for NHL5 mortars (values reported in [39, 152, 156, 157])



metastable phases of calcium carbonate are formed (vaterite and to a lesser extent aragonite). These metastable phases are transformed into the stable phase, calcite, through processes of dissolution–precipitation, both homogeneous and heterogeneous [86]. The process of formation of nanolime is carried out in alcoholic environments in which the formation of amorphous or metastable phases is promoted. Its transformation into the calcite phase, the stable one, is carried out after several months. Some authors [75] have shown that this time can be reduced if the alcoholic medium is eliminated, for example by means of a heating process. From Martínez-Ramírez et al. [87] it can be concluded that there is no relationship between carbonation depth and the type of calcium carbonate polymorph.

2.3 Influence on the performance of mortars

2.3.1 Shrinkage

Generally, mortars with higher mixing water content undergo a much higher drying shrinkage in the first few hours. The low cohesion of weak mortars also may increase shrinkage. So, although the general rule is that higher contents of binder generate higher shrinkage, it may also happen that mortars with low binder

contents, in certain cases, show higher shrinkage, due to low resistance to deformation [32]. However, it is important to notice that high shrinkage with high deformability may not lead to cracks, as deformation may be enough to release stress, and that other factors, such as tensile strength and relaxation, have also a role [88]. Additionally, the extent of the resulting micro-cracking depends on the external geometrical restraints that may condition deformability. Hence, cracking due to drying shrinkage depends on the exposure conditions, on the aggregate content and properties (mechanical and thermal), on the characteristics of the porous network and on external deformation restriction, such as adhesion to a rigid background [76, 77].

According to Arizzi et al. [32], shrinkage cracking in hydraulic lime mortars is related with:

1. the amount of mixing water, which shows its effect during the first few hours of drying; higher water content involves a much higher shrinkage in the first few hours, in a period when mechanical characteristics are not much developed to resist the generated stresses; this means that the kinetics of drying has also a role in cracking [76, 88];
2. the internal cohesion of the mortar, which can also be referred as deformability. This effect may help

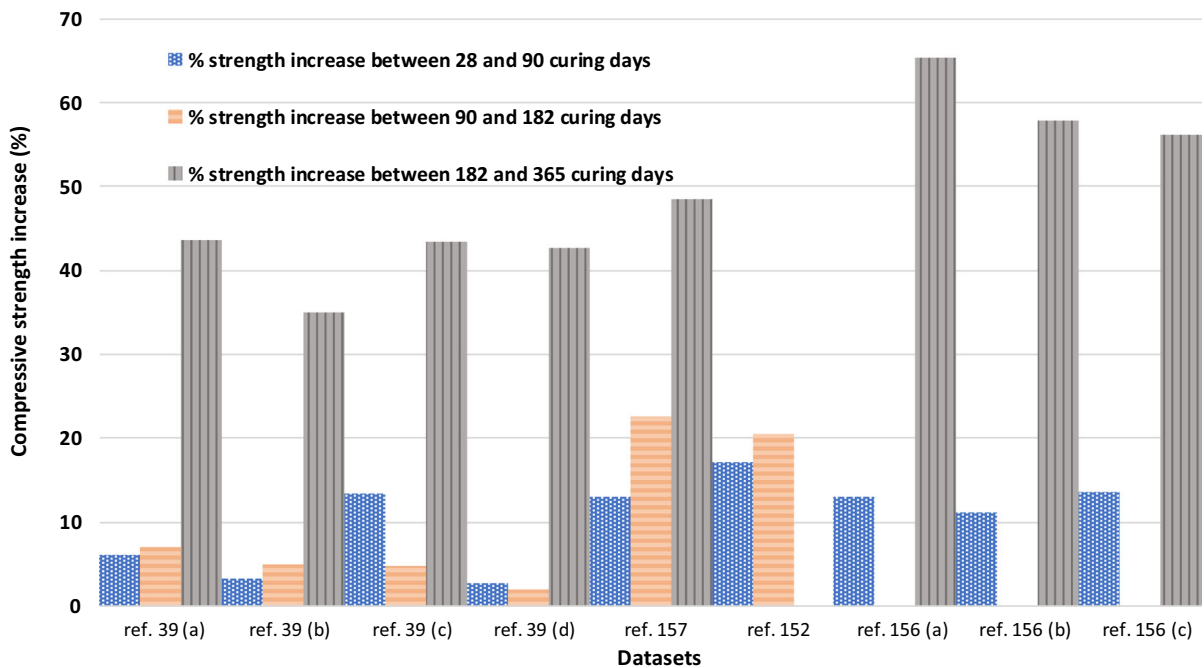


Fig. 4 Percentage of compressive strength increase with respect to the final measured strength at different periods of curing time (values reported in [39, 152, 156, 157])

to explain why the highest shrinkage values appear in pure lime-based mortars [60].

2.3.2 Cracking and adhesion

The durability of coating mortars and renders is strongly affected by cracking due to drying shrinkage. In fact, diffusivity and permeability, to water and to different solutions and other products in vapour and liquid state, may increase due to cracking by several orders of magnitude. Cracking may also create debonding.

The main modes of failure in mortar/substrate systems are [89]: tensile cracking through the mortar thickness, and peeling or shearing at the interface between both materials. The main sources of cracking are stresses induced by restrained drying shrinkage [88, 89]. Cracking may be raised by severe drying conditions. The development at early age of this stress state is overly complex. It is strongly heterogeneous in the mortar thickness due to the combination of several phenomena, such as hydration, drying, evolution of mechanical properties, and creep. Shear stresses generated at the interface between the two materials

affect adhesion and eventually may produce debonding.

Cracking due to drying of coating mortars is highly dependent on the boundary conditions (external RH, wind velocity, etc.) and the substrate (roughness, Young modulus, etc.). The adhesion of lime-based mortars to a substrate depends on the moisture and open porosity in the substrate/mortar interface [81] (Fig. 1), provided that materials have been applied by good and comparable workmanship.

2.3.3 Mechanical and hygric characteristics

For hydraulic lime mortars, the control of drying is a key parameter to get mechanically resistant mortars. Concerning pure air lime mortars, the effects are more complex: some moisture is needed for CO₂ dissolution, but saturation hinders carbonation reactions, so intermediate conditions are needed.

There is an interdependence of properties that requires a careful balance. All the mechanical characteristics, including the dynamic modulus of elasticity, are dependent on water/binder ratio (decreasing with w/b increase) and on binder/aggregate ratio

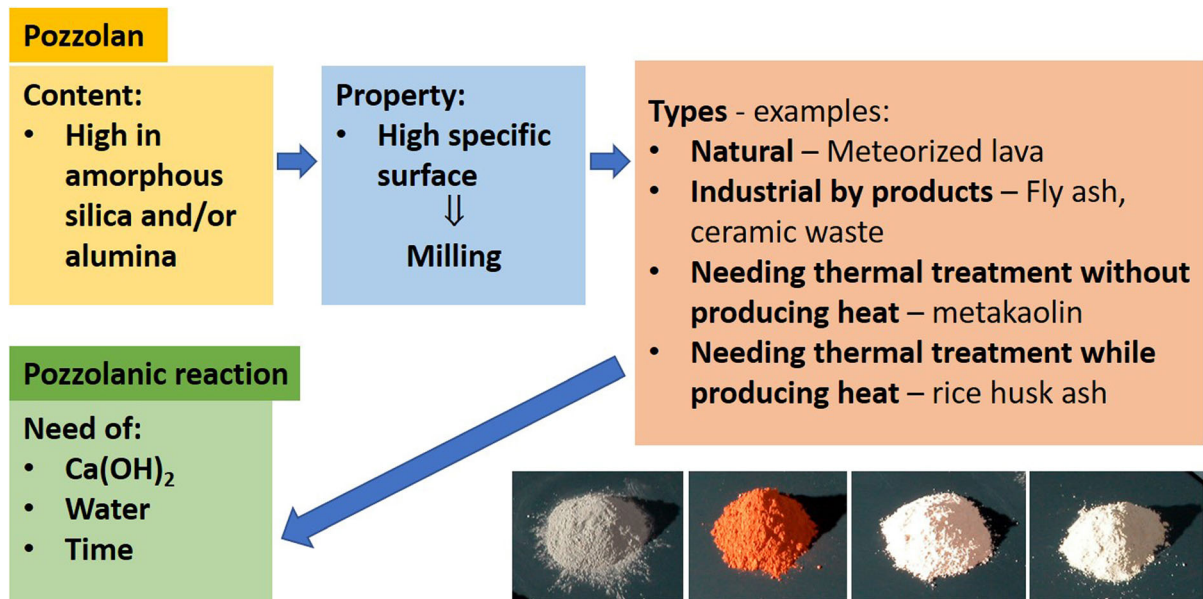


Fig. 5 Characteristics, types and examples of pozzolans and pozzolanic reaction

(increasing with b/a increase). Additionally, in all cases, the mechanical properties also increase with moisture removal by the drying during hardening [77], due to reduction of porosity and compaction of the solid structure. For similar reasons, the mechanical characteristics were also found to be increased, when the mortars are applied onto porous substrates [70]. However, drying with high temperature and high rate is expected to cause significant internal moisture decrease, producing microstructural modification due to incomplete hydration, and shrinkage cracking in the mortar, which result in higher porosity. Thus, such adverse drying conditions may result in reduction of the mechanical characteristics.

The development of properties of mortars is decisively dependent on the curing conditions as they affect the pozzolanic reaction and carbonation of mortars [74]. Air lime mortars cured in humid conditions without access of air (or CO_2) and saturated in water remain uncarbonated. Therefore, those mortars develop only minimal compressive strength. Mortars shrink considerably due to drying when they are cured in dry air conditions (RH 65%); however, if severe cracking does not occur, they achieve satisfactory values of compressive strength after full carbonation. Semidry conditions with access of air seem to be the most favourable for carbonation and hardening of lime mortars.

The water absorption coefficient of air lime mortars experiments a decrease when they are applied on absorbent substrates, due to the reduction of porosity, except in the case of pre-dosed mortars modified with water-repellent admixtures [70]. Water vapour permeability was also found to be reduced when applied to porous substrates [70].

The volume and type of porosity is very influenced by drying parameters: rate of drying and temperature, which may cause reduction of porosity or, on the opposite, produce micro-cracking increasing coarse porosity. Different drying mechanisms (evaporation, suction of the substrate and autogenous drying) also produce different pore size distribution [70]. Thus, the drying conditions and types (evaporation, autogenous, absorption by the substrate) change the microstructure and, consequently, affect water transport properties: liquid absorption, vapour diffusion and drying in the hardened state (Fig. 1).

Lime–pozzolan mortars and especially those from lime–metakaolin mixtures cannot be effectively used without precise knowledge about drying conditions. Mortars with this composition do not develop their binding potential in dry conditions. However, they achieve good performance properties in humid conditions [90]. The positive pozzolanic potential of these materials is critically affected by the environmental conditions under which mortars are cured.

2.3.4 Atmospheric aggressive compounds and their effects on durability

A main part of the durability of the lime-based mortars is related to the ingress of atmospheric aggressive compounds (rain water, SO₂, NO₂, etc.) that is causally related to porosity. Drying conditions affect shrinkage and porosity and may cause cracking and debonding, may promote the ingress of atmospheric agents and are thus critical for the durability of mortars. Since this influence is significantly different for hydraulic and non-hydraulic mortars, the optimization of the curing conditions for the drying control must be related to the type of binder.

Atmospheric pollutants, SO₂ and NO_x, reacts with portlandite producing soluble salts (calcium sulfate and nitrate) which cause dissolution-crystallization cycles depending on external conditions (RH and T), which can lead to efflorescence.

On the other hand, water also plays an important role in accelerating the reaction of mortars with atmospheric pollutants, as well as being capable of producing freeze–thaw problems. Uncarbonated air lime mortars show no resistance to frost, whereas after full carbonation they achieve reasonable frost resistance due to the high porosity of the carbonated lime mortar. Lime-pozzolans mortars also achieved good durability in humid conditions as water permeability is reduced due to their low porosity [90].

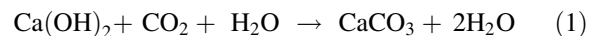
3 Carbonation

Carbonation is responsible for the setting and hardening of lime-based mortars, and it consists in a series of chemical reactions between calcium hydroxide and atmospheric carbon dioxide, to form calcium carbonate [91, 92]. The several stages of lime production and utilization are strongly correlated through the so-called “lime cycle”, which leads to a final product, CaCO₃, chemically equivalent to the starting limestone raw material [93]. The production stages of lime start with the calcination of pure limestones (between 700 and 900 °C), which allow the formation of calcium oxide (CaO, quicklime) and the release of CO₂. The obtained quicklime, highly metastable, is then subjected to a forced hydration process, slaking, through the submersion or aspersion of water, obtaining calcium hydroxide (Ca(OH)₂, portlandite), which

is the mineral constituent of building lime. The amount of water should be either stoichiometric, obtaining a powder of hydrated lime, or in excess, obtaining a slurry called lime putty. Portlandite subsequently reacts with atmospheric CO₂, forming CaCO₃ crystals and closing the cycle. The proposed array of reaction processes is equally applicable to the magnesian component of dolomitic limes, in case of calcination of dolostones/dolomitic limestones. In this case, the calcination process produces a combination of quicklime and magnesium oxide (MgO, periclase), while the slaking produces a combination of portlandite and magnesium hydroxide (Mg(OH)₂, brucite), and the carbonation a mix of calcium and magnesium carbonates. For sake of clarity, only the most diffuse high-calcic limes will be taken into consideration in the next sections, tackling the peculiarities of dolomitic lime mortars in Sect. 3.5.

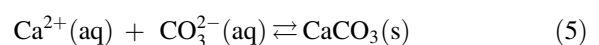
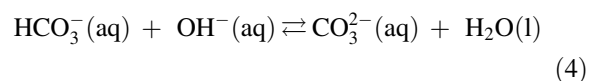
3.1 Reactions of carbonation

The process of carbonation can be described through the simplified carbonation reaction (1):



This is controlled by diffusion-related factors and by the atmospheric CO₂ concentration, so lime mortar carbonation generally proceeds gradually, according to an interfacial process and only after an initial dormant phase during which a partial drying occurs until reaching RH between 40 and 80%, necessary to start CO₂ diffusion and dissolution within the partially-filled pore network of the material [93].

The carbonation process can be subdivided in different reaction steps: dissolution of CO₂ into the aqueous medium (2), interaction of CO₂ with hydroxyl ions to form hydrogen-carbonate and carbonate ions (3 and 4), and final reaction of the carbonate ions with Ca²⁺ (5) [93]:



In the proposed array of chemical reactions, reaction 3 is the rate-controlling step, being slower with respect to reaction 4, which is practically instantaneous. Starting from the proposed carbonation model, an experimental study [94] proved that lime carbonation proceeds in three stages. Stage I proceeds under a chemical-reaction controlled regime, due to the limited CO₂ diffusion through the saturated pore network. Furthermore, the initial CO₂ uptake promotes a rapid carbonation on the surfaces of portlandite crystals, forming a passivating layer of amorphous CaCO₃ that facilitates the instauration of a dormant period. The reactivation of the carbonation process, which proceeds rapidly during stage II, is promoted both by the conversion of amorphous CaCO₃ into calcite and by the drying effect, which favors the diffusion of CO₂ within the system. Such stage is strictly diffusion controlled. The final stage III takes place after the completion of surface carbonation, with the transition to a diffusion-controlled regime significantly hindered by the reduced permeability of the carbonated layer.

3.2 Kinetics of carbonation

Experimental studies and building practices demonstrated that carbonation is a slow reaction process proceeding until either all calcium hydroxide has reacted, or capillary water is evaporated. The progression of the carbonation reaction can be expressed through a simplified interfacial process ruled by first Fick law of diffusion [95], causing the development of the so-called carbonation front according to the following equation:

$$x = K * \sqrt{t} \quad (6)$$

where x is the distance between the surface and the carbonation front, t is the reaction time and K is a constant related to the chemical-physical parameters of the carbonating system (e.g. lime reactivity, CO₂ partial pressure, water to binder ratio and RH, permeability of the system). Furthermore, a fast progression of the carbonation front may be promoted by the instauration of specific catalytic factors, such as the formation of liquid-like water vapor adsorption layers at RH values greater than 0.7, enhancing reaction processes between porous calcium hydroxide particles and carbon dioxide [96]. The reliability of the

equation has been proved by several experimental studies [92, 97, 98]. Nevertheless, simple empirical measurements for the monitoring of carbonation demonstrated the absence of a sharp carbonation boundary, confirming rather the occurrence of volumes of material of high and low carbonation level upon the global progression of the reaction process [99]. In this perspective, the progression of the carbonation process can be practically described through an asymptotic function [100]. According to this model, the degree of carbonation varies between 40 and 60% close to the carbonation front, decreasing in a nearly linear manner down to 0% ahead of the layer of maximum carbonation, with thickness values strongly influenced by compositional and textural characteristics of the binders. More precise parametrizations of the actual kinetics of the carbonation process can be extrapolated by experimental studies on nanolimes [86, 101]. As for the crystallization pathways, Rodriguez-Navarro et al. [86] demonstrated that the carbonation process starts with the formation of ACC, subsequently transformed into metastable vaterite (and minor aragonite) via a dissolution-precipitation process, followed by non-classical nanoparticle-mediated crystal growth. Then, stable calcite precipitates after dissolution of the metastable polymorphs. All these phase transformations follow first order kinetics, where the rate controlling step is the amount of undissolved parent phase. Concerning the type of kinetic model, Camerini et al. [101] demonstrated that the Boundary Nucleation and Growth Model (BNGM) constitutes the best choice to describe the carbonation process, allowing both to consider the separate contribution of the nucleation and growth of calcium carbonate phases, and to take into account the role of the surface area of the particles in the transformation of Ca(OH)₂ into CaCO₃. Calculated activation energies (E_a) for the carbonation process on four different nanolime systems, extrapolated applying the aforementioned model, range from 31.4 to 59.6 kJ mol⁻¹.

3.3 Factors affecting the carbonation rate

3.3.1 Water amount (relative humidity) and CO₂

The amount of water, temperature and CO₂ partial pressure are the key factors to be considered along the reaction path [102]. As for the former, the presence of



enough water is critical to allow both calcium hydroxide dissolution and atmospheric CO₂ uptake but, at the same time, high water contents hinder CO₂ diffusion [103, 104]. As previously stated, it has been determined that RH comprised between 40 and 80% are ideal to allow adequate dissolution and diffusion processes of CO₂ in pore solution [6]. As for CO₂, there is general agreement in observing an increase in the speed and rate of carbonation at increasing values of available CO₂ within the system [103]. Nevertheless, it has been observed that heat generated during rapid reaction processes promoted by high CO₂ availability is responsible for the evaporation of water in pore solution, thus hindering the carbonation rate [105, 106]. Other system conditions-related factors influencing the progression of the carbonation process are the filler concentration, slowing down CO₂ diffusion at increasing values [107], the characteristics of the masonry, such as thickness and composition, influencing the permeability of the system [97, 100], and the degradation of mortars, changing compositional and textural characteristics of the composites [108]. The factors and optimal conditions for the lime mortars carbonation according to the literature are summarized in Table 1. Furthermore, it is worth mentioning a recent study by Ergenç and Fort [109], which determined the optimal conditions to promote a representative accelerated carbonation of lime-based mortars in climatic chamber: the best results were obtained with a temperature of 20 °C, a RH of 60% and a CO₂ concentration of 1600 ppm.

3.3.2 Particle size and crystallographic characteristics of the lime: influence of the burning and slaking processes

Cizer et al. [94] demonstrated that the reaction rate and the amount of CO₂ uptake are not proportional to the initial CO₂ concentration, but they are more influenced by the crystallographic and dimensional characteristics of lime. The smaller the particles of portlandite, the faster is the transition from stage I to stage II of the carbonation process, due to their higher solubility and consequent reaching of higher levels of supersaturation during the chemical reaction processes, leading to a higher nucleation density of the calcite crystals.

Such experimental evidence has direct consequences in the optimization of the production stages of lime cycle, to obtain better nanostructured, and thus

more reactive, limes. The two stages that allow higher operative margins are the calcination and the slaking process.

As for the calcination, the best quicklime reactivity is obtained through the adoption of firing temperatures around 900 °C, with a progressive loss of reactivity at increasing values [106]. The samples calcined at 900 °C are characterized by a higher total cumulative volume, porosity and specific surface area. Furthermore, they are characterized by higher temperature increase and higher expansion during slaking. Rodriguez-Navarro et al. [114] unveiled more detailed mineralogical insights on the factors influencing this reactivity, demonstrating the nanostructural arrangement of quicklime particles during and after firing. The reaction starts at 600 °C with the superficial formation of pockets of oriented CaO crystals, and reaches a full conversion at 850 °C. At higher temperatures, relevant sintering phenomena of the CaO crystals take place, with the development at 1000 °C of equidimensional, micrometer-sized CaO grains characterized by the occurrence of straight triple boundaries as well as neck contacts, typical features of the sintering process [115]. Concerning the specific surface area, highest values were obtained at 750 °C, with a progressive reduction at higher temperatures, indicating a reduced triggering of the sintering processes even at values lower than 1000 °C. As for the porosity, values close to the theoretical maximum of 54.2% were yielded at 900 °C, with a progressive decrease at higher temperatures, clearly indicating an association of sintering and shrinking processes [116]. In general, the best temperature interval in terms of calcination progression, specific surface area, overall porosity and prevention of sintering phenomena is comprised between 850 °C and 900 °C.

Concerning the optimization of the slaking process, lime aging by immersion in water in order to obtain a high-quality slaked lime was known and parametrized since ancient times, such as 3 years of lime curing within water ponds prescribed by Plinius the Elder in the Fifth Book of its *Naturalis Historia* [117]. Several studies investigated the microstructural reasons for such a long preparation [110–112], demonstrating a clear decrease in portlandite crystallinity upon aging, contributing to a general surface area increase.

From a crystallographic point of view, this is due to a progressive transition from large micrometric



prismatic portlandite crystals to hexagonal platelike, submicrometric ones. This experimental evidence is in contrast with the generally accepted Ostwald ripening theory [118], i.e. development of larger crystals at the expense of the smaller ones to attain the lowest total surface energy of the system. This phenomenon is justified taking into account a preferential dissolution of prismatic {100} faces of the large portlandite crystals due to a higher surface energy with respect to the basal pinacoid ones, facilitating the development of {0001} faces upon aging [110–112]. This is strictly related to the crystal structure of calcium hydroxide, constituted of layers of $\text{Ca}(\text{OH})_2$ having hexagonal symmetry, bonded together by weak van der Waals forces, resulting in a perfect basal cleavage [119].

The observed reduction in particle size and peculiar shapes have direct consequences on the rheological properties of fresh putties and mortars [120, 121], namely a net plasticity increment due to a greater capacity to absorb water, a higher thixotropic behavior and a yield stress increment. As for the hardening, a faster overall carbonation for the materials prepared with the most aged binders has been demonstrated [121], with a development of smaller calcite crystals, more interlocked and arranged on a rigid, three-dimensional structure. Furthermore, the binding matrices produced by carbonation of the aged putties show peculiar microstructural features of alternating calcite-rich and portlandite-rich rings, similar to the so-called Liesegang rings forming on far-from-equilibrium precipitating systems [111, 122, 123]. On the contrary, non-aged lime putties with large portlandite crystals of lower solubility are characterized by limited calcite precipitation at low supersaturation ratios, typical for closer-to-equilibrium diffusion-limited systems. In this case, the carbonation process is gradual and homogeneous, from the surface toward the sample core.

3.4 Carbonation rates on lime mortars upon aging

The parametrization of the carbonation processes of lime-based mortars needs to consider the final degree of carbonation reached by the systems at the end of the reaction phenomena. The study of ancient mortars gives insights on materials aged for centuries. There is general agreement in scientific literature on the impossibility to reach 100% carbonation levels, with medium values generally attested between 80 and 90% for mortars close to the surface exposed to the

atmosphere [124–127]. This is in accordance with experimental studies on modern mortars, reporting final carbonation values comprised between 80 and 92% [92, 111], influenced by lime putty quality, the type of aggregates and the progressive loss of permeability of the masonry systems upon aging.

3.5 Carbonation and performance of dolomitic lime mortars

In fresh state, the properties of the dolomitic lime mortars are strongly influenced by the mixing water content of the paste, like in the calcitic lime mortars. In the works by Arizzi et al. [128] and Arizzi and Cultrone [34] it has been reported that dolomitic limes confer a higher plasticity to the fresh pastes as compared with calcitic limes. The use of dolomitic lime in mortars generally led to a higher mixing water demand, although this parameter is dependent on the specific surface area and micropore volume of the limes and can be thus variable as a function of the production conditions. Arizzi and Cultrone [34] state that since brucite particles are thinner and larger than portlandite ones, a greater fineness may be reasonably expected in dry dolomitic limes.

No strong differences are observed in the hardened performance of mortars as a function of the original composition of the air lime (calcitic or dolomitic) [2, 33, 129]. Similar final mechanical strengths were achieved in samples tested along 1 curing year, although final strengths were slightly higher for dolomitic mortars [33]. According to Chever et al. [35], providing an appropriate Mg-lime production (absence of over/underburnt and/or unslaked particles), mechanical properties could reach values like those obtained in natural, feebly hydraulic lime mortars. The age at which dolomitic lime-based mortars reach their maximum strength is ca. 91 days (aggregates with siliceous composition) or ca. 365 days (calcareous aggregates) [33]. Figure 2 presents the values of 20 published datasets of compressive strengths of dolomitic lime mortars (with diverse binder/aggregate ratios, which explains the variability) [33–36, 129, 130]. The average values as a function of the testing age are 1.41 MPa (28 days), 2.31 MPa (90 days) and 4.49 MPa (365 days). These values might be compared with those obtained by Lanás and Alvarez [2] in calcitic air lime mortars (average values of 1.13 MPa after 28 days, 1.62 MPa after 90 days, and 3.08 MPa after 365 days).

The influence of the raw dolomitic material is however of the utmost importance. Whereas CaO hydrates at high rate in the presence of water, MgO shows a slower rate of hydration, which is strongly influenced by the particle size distribution and by stirring [131]. Other works showed that the calcination process of the raw dolomitic limestone and the slaking process (atmospheric environment, excess of water, CO₂ presence ...) yielded dolomitic limes with different behavior, which gave rise to the formation of different magnesium carbonates after hardening (hydromagnesite, nesquehonite, amorphous carbonates,...) [132]. Whereas in ancient mortars the presence of dolomite was evident together with poorly crystalline phases of other magnesium carbonates, the formation of phases on repair mortars obtained from calcination of dolomitic limestone matches a different pattern [133–137]. The control of burning and slaking processes seems to be of paramount importance for dolomitic lime mortars [35].

The monitoring of the different phases formed in dolomitic lime mortars showed that the brucite amount is kept almost constant over time. As possible explanations to this fact, Lanas et al. [33] argued the very slow carbonation process and/or a dedolomitization reaction (alkali-carbonate reaction, ACR) between Ca(OH)₂ and dolomite present in the specimens [138, 139]. The newly formed calcite through ACR and the brucite crystallization improve the strength further than similar calcitic air lime-based mortars. Štukovnik et al. [140] also found an increase in strength due to the ACRs inside the air lime mortar with dolomitic aggregates. This strength rise is ascribed to the formation of secondary CaCO₃ that fills pores inside the lime binder. The calcite formation is due to two reactions: (a) release of carbonate ions during the dedolomitization process and their reaction with the Ca²⁺ ions of the portlandite; (b) the CaCO₃ dissolution/precipitation cycle during the dedolomitization process inside the dolomite aggregate grain, owing to the gradients of the carbonate and hydrogencarbonate ions that arise inside or outside the aggregate.

4 Hydration

The hydration as a mechanism for binding action in lime-based binders can be invoked when a certain hydraulic character of the matrices is ascertained. The

term hydraulic could be used in connection with the capacity of hardening (and thus binding) when water is added to the dry binding system. This mechanism is of interest for both hydraulic-lime (NHL or lime-pozzolan) and lime-cement binders.

4.1 Lime-based mortars with hydraulic properties

A hydraulic lime-based binder is obtained due to the presence of different materials that confer it the hydraulic properties. The content of impurities in the raw limestone, silica (SiO₂) and alumina (Al₂O₃) mainly, is responsible for this effect [141, 142]. A lime with hydraulic properties [41] can be produced burning at 900–1250 °C limestones with a high content of clays (6.5–20%) (in that case the final product would be a Natural Hydraulic Lime, NHL) or mixing clay minerals with finely ground pure limestones [143] or with other materials. An optimal burning temperature depends on the raw material composition [144]. The reaction between the lime and SiO₂ and Al₂O₃ leads to the formation of calcium silicates and aluminates. The hydration of these compounds forms the hydrated compounds, C–S–H and C–A–H, which provides strength to the mortar [145].

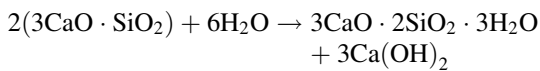
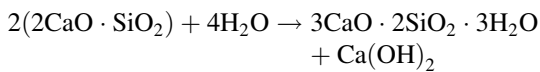
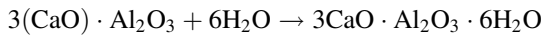
During the production of a hydraulic lime, burning limestone with siliceous impurities, the final temperature of burning should not exceed 1250 °C, because sintering occurs at higher temperatures. The different temperatures of burning as well as the content in siliceous materials in raw materials lead to different composition of the hydraulic phases between NHL and cement and have an influence on the final properties of the binder. Whilst in cement calcium silicates (mainly C₃S) and calcium aluminates (C₃A and C₄AF) are formed during sintering, in NHL larnite (a C₂S analogue) is the major hydraulic phase together with a lower amount of gehlenite (C₂AS) [146–148]. The presence of gehlenite indicates the lower temperature reached in the burning process of NHL. These compounds often appear in a poor crystalline form, they are usually present in limited concentrations and, when analyzed by X-ray diffraction, their characteristic peaks tend to overlap [149]. C₃S, C₃A and C₄AF may be also detected in NHL [150], in small amounts, due to a local overheating in the kiln. Calcium hydroxide (CH) also appears. In cement clinker, free CaO is combined during sintering, and no free CH is



checked. Gehlenite does not appear in the final cement either [151].

4.1.1 Reactions of hydration—Influence of different factors

Hydration reactions of the anhydrous calcium silicates and aluminates are usually described as follows, depending on the final composition of the binder [152]:



The hydration of C_2S (belite) takes place at long times (around 6 months) whereas C_3S and C_3A hydrate at a remarkably high speed. A rapid strength gain is observed in systems with C_3S (alite) due to the hydration of this hydraulic component. At 28 days, belite attains approximately 10% of the strength (weight for weight) of alite [153]. The strength development ascribed to C_2S hydration stretches over 1 year.

The water/binder ratio and the curing conditions can have a severe influence on the rate of hydration, especially if the competition between carbonation vs. hydration is considered. This competition will be tackled below.

4.1.2 Effect of the hydration on the hardening of hydraulic lime mortars

Lanas et al. [39] studied the mechanical performance of NHL-5 mortars cured under conditions of 60% RH and 20 °C and showed three different stages, depending on the curing ages:

1. In the early ages (up to 28 days), mortars with high lime content gain 50% of their maximum value of strength. As C_3S hydrates quickly, the strong strength increment observed at early ages can be attributed to its hydration [153]. As in either NHL or HL mortars, the amount of C_3A is expected to be, if any, low, its role should be considered

negligible. This was also confirmed by Garijo et al. [154] with a set of NHL mortars.

2. At medium term (28–182 days, approximately), the compressive strength of mortars only increases slightly owing to the following reasons: (1) the C_3S hydration could be practically finished; (2) the slight influence of C_2S hydration, because the main part of its contribution occurs from 28 days onwards, with maxima values at long-term ages [155]; (3) carbonation is not significant in terms of extent and strength contribution (which is always lower than that of the hydraulic components).
3. At long-term curing times (182–365 days), compressive strengths of mortars with large binder/aggregate ratios increase again due to the contribution of C_2S hydration to the strength. In addition, the carbonation degree can reach significant values and thus its contribution to the strength can be clearly checked.

Some datasets of values published for NHL mortars have been re-analyzed. Figure 3 depicts nine datasets (compressive strengths along curing time of mortars prepared with standard NHL 5), selected from papers in which at least measurements at three of the 28, 90, 182 and 365 curing ages were reported [39, 152, 156, 157] (extrapolating the values in ref. 156 from 270 to 365 curing days).

Some conclusions can be drawn:

- The graphical representation in Fig. 3 shows that the strength increment between 28 days and half a year is, in general, moderate, in line with the conclusions by Garijo et al. [154], similarly obtained for mortars prepared with NHL 3.5.
- On average, NHL mortars gained 51% of their final measured strength during the first 28 days.
- The noticeable effect of the long-term curing in the NHL mortars can be seen in Fig. 4. Some data are not available due to the absence of these values in the articles. The percentages of strength contribution of the period 182–365 days with respect to the final measured strength are larger than those of the mid-term (28–90 and 90–182 days). For almost all the reported datasets, a contribution of more than 40% of the final strength was observed for the period between 182 and 365 days (combined effect of C_2S hydration and carbonation).

Apostolopoulou et al. [158], using artificial neural networks computing techniques, studied the significant influence of the mix design parameters in the compressive strengths of available data published about hydraulic lime mortars. The influence of these factors explains the variability in the values of the final strengths.

4.2 Lime-cement mortars

As mentioned before, RILEM TC LHS-277 agreed that lime-cement binders being dealt with are compositions with less than 30% cement by weight in the binder. The types of cement that are normally incorporated in such systems may be different categories of hydraulic cements, blended hydraulic cements, pozzolanic cements, Portland cements and, in some cases, slag cements [159, 160].

In most cases, however, research and field work are carried out using Portland cement and either hydrated lime powder (commercially available) [48, 79, 161–164].

4.2.1 Hydration of cement

This process has been extensively studied in the scientific literature. Cement hydration involves different coupled physico-chemical processes detailed in the work by Bullard et al. [165]. Hydration of the most straightforward calcium silicate and aluminate systems, C_3S (alite), C_2S (belite) and C_3A and C_4AF leads to formation of amorphous C–S–H (calcium silicate hydrate), CH (calcium hydroxide), calcium aluminates hydrates and ettringite [165, 166]. Isothermal calorimetry is useful to ascertain the different stages taking place during the hydration of the anhydrous systems, which are usually initial reaction (beginning immediately after the wetting and with an intense heat release because the dissolution of the active compounds), period of slow reaction, acceleration stage with C–S–H formation, and deceleration period. The work by Bullard et al. provides insights into the hypotheses and mechanisms to explain the different periods. The precipitation of C–S–H occupies a significant portion of hydrated cement, by volume [167]. The resulting product may vary in terms of its bulk density and morphology based on the temperature of the reaction [168]. The network of C–S–H crystallites often encapsulate large, irregular shaped

agglomerates of portlandite, which are formed as a by-product in the reaction and tend to grow preferentially in clusters on certain nuclei of the alite crystals [169, 170]. Together, the structure of C–S–H and CH form strong connections with the solid phase, binding discrete compounds into a cohesive whole and consequently contributing to the overall strength and stiffness of hydrated cement.

It is well established that the greater the RH, the more efficient is cement hydration. RH must not fall below 80% to promote cement hydration [171]. With regard to effect of temperature, an increase in curing temperature causes an increase in speed of the initial rate of hydration [172]. However, this does not directly imply beneficial effects at the macro scale. Higher temperatures are reported to lead to a more heterogeneous distribution of hydration products and more coarse porosity of the hydrated composite, potentially causing lower values of strength and stiffness after the initial few days of curing [172]. As the temperature of hydration increases, the resulting C–S–H formed undergoes a greater degree of polymerization of its silicate chains, a decrease in its amount of structurally bound water and a consequent increase in its apparent density [173]. Lower temperatures of reaction lead to a slower hydration, allowing more time for ions in the solution to dissolve, corresponding hydrates to precipitate and distribute more evenly. At 5 °C, the C–S–H crystallites present lower coarse porosity and better interlocking of different phases [174]. At a macro-scale this would translate to lower temperatures causing relatively slower evolution of strength and stiffness initially, but leading to higher mechanical properties by the end of the curing period, as a result of more homogenous distribution of hydrated products [175].

4.2.2 Simultaneous effect of carbonation and hydration in lime-cement mortars

Hardening in lime-cement systems occurs as a combination of cement hydration and lime carbonation, with the former being the faster and more dominant reaction [47]. Hydrated phases formed in the combined system are the same AFm (shorthand for family of hydrated calcium aluminate phases) and C–S–H phases that are found in hydrated cement, but the formation of C–A–H phase is also reported [161]. The C–A–H phase has been observed in hydrated lime-



cement pastes but is absent in cement only pastes [161], and occurs as hexagonal plate-like crystals with fine granular aggregates of size less than 1 μm , which may also occur as irregular or fine spherical particles [176]. The C–A–H phase may further react with carbonate ions and lead to the formation of C–A–C–H (calcium carboaluminate hydrate), the presence of which (through XRD) indicates the presence of additional lime in cement hydration [177]. However, it must be highlighted that the presence of low quantity of limestone (\sim up to 5%) in cement, also leads to the formation of C–A–C–H phases formed due to the reaction of carbonate ions with C₃A and AFm phases [178, 179]. Within this margin of 5%, lower levels of calcite presence, leads to the formation of hemicarboaluminates, which get replaced by monocarboaluminates as the level of calcite increases [180]. This is important because only the latter AFm phase, namely calcium monocarboaluminate is detectable in well hydrated cement [178]. Beyond this threshold, excess calcite has been reported to mostly act as inert filler in cement hydration [180].

The main CaCO₃ polymorphs formed because of carbonation of calcium hydroxide, are calcite (scalenohedral, rhombohedral and prismatic habits), aragonite (spotted as needles) and polycrystalline vaterite (spotted in spherical shapes) [161], with the first one being the most stable and the last one being the least stable from a thermodynamic point of view [181, 182]. It is reported that, in stoichiometric conditions, rhombohedral formation is favoured [161]. In non-stoichiometric conditions however, scalenohedral formation is preferred when Ca²⁺ to CO₃²⁻ ratio ≥ 1.2 , and the rhombohedral form is favoured in low ratios of Ca²⁺ to CO₃²⁻ or excess of CO₃²⁻ [183, 184]. Furthermore, the modification of scalenohedral form to rhombohedral reportedly occurs in lime-cement systems due to the phenomenon of dissolution, followed by reprecipitation of calcite. The reaction of carbonation initially takes place in a calcium-rich environment and promotes the growth of scalenohedral structures. At this stage, the amount of carbon dioxide in the specimen is restricted due to its low diffusivity in water, as the surface of the lime-cement mortar has a layer of moisture on it [168]. With the progress of the reaction and corresponding release of heat, this film of water evaporates enabling the diffusion of carbon dioxide into the pores and subsequently reducing the pH value of the

environment [184]. SEM images have shown that this reduction in pH corrodes and disintegrates the existing scalenohedral structure, leading to the formation of rhombohedral crystals on its faces (nanometer sized). These calcite crystals, which reprecipitate, have extremely sharp edges and form along the edges of the carbonated matrix [85, 161]. Since cement hydration also produces portlandite, the compounds formed because of varying kinetics of lime carbonation and cement hydration are highly dependent on the amount of moisture present in the curing conditions.

Another aspect that merits discussion in a combined system of lime and cement is carbonation of hydrated phases. This is reported to cause decalcification of the corresponding calcium silicate hydrates and calcium aluminate hydrates [185]. The decalcification of hydrated phases may lead to the formation of hydrous silica and alumina highly polymerized, but the precise nature of these compounds is unknown and requires further investigation [186–188]. Upon complete decalcification of the hydrated phases and their complete destruction, the precipitation of rhombohedral calcite crystals and acicular pyramidal aragonite crystals has been observed [161]. The resulting carbonated matrix is poor and full of cracks. Cizer [161] reports, however, that regardless of the curing condition, amount of CO₂ in the curing environment and decalcification of the hydrated phases, long term development of strength in lime-cement systems (mortars in particular) is not affected. The reason proposed is that the carbonation of free Ca(OH)₂ and anhydrous compounds in cement serve as compensation.

When hardening in a material occurs because of a combination of carbonation and hydration, RH plays the most important role in curing conditions and can impact short- and long-term mechanical properties of the resulting mortar or grout. Cizer [161] performed an extensive study about different moisture curing conditions in lime-cement systems (at 20 °C) and the relevant findings may be listed as follows:

Regardless of moisture content, in atmospheric conditions, cement hydration always occurs before carbonation of free lime.

RH in curing influences the degree of hydration and carbonation. RH ca. 93% renders cement hydration almost complete within the first 28 days, whereas RH ca. 60% facilitates carbonation of free lime 7 days onward.



Regardless of RH being 90% or 60%, lime-cement systems exhibit long term strength development (mechanical strength was measured up to 360 days).

The work also states that, for similar proportions, choosing between lime putty and hydrated lime in a lime-cement system could have significant consequences on the mechanical properties of the resulting lime-cement mortar. Lime putty is expected to result in lower mechanical strength and higher porosity and shrinkage as compared to hydrated lime. This may be attributed to lime putty having higher viscosity and water retention than hydrated lime because of differences in particle shape [189]. While decalcification of hydrated phases due to carbonation was observed, no impact on mechanical strength was reported. On the contrary, significant gains were recorded, the reason for which has been attributed to almost full carbonation of lime in the long term, coupled with carbonation of anhydrous cement compounds [161]. With respect to setting time, addition of lime is reported to cause earlier setting of cement pastes, by reducing the induction period typically associated with cement hydration [190]. Fourmentin et al. [190] presume that this happens due to the high specific surface area of lime. Due to the availability of larger surface area, C–S–H precipitation is expected to occur on portlandite crystals in the pores of the cement paste instead of only occurring on the surface of the grains. The acceleration of the setting time, however, is shown to be negligible beyond a critical concentration of lime fraction (30% by volume) in the mix.

5 Pozzolanic reaction

Pozzolans are materials with high contents on amorphous alumina and/or silica with high specific surface area. Pozzolans depend on other components to be reactive: they do not possess binding ability by themselves. Composition and fineness are the key factors [191, 192].

Natural pozzolans mainly result from meteorized lava that is milled to become fine. Artificial pozzolans can come from a raw material, such as a clay, but needing a thermal treatment: for example, metakaolin is obtained from kaolin fired at 600–900 °C for at least 30 min [193]. By the treatment the kaolinite mineral ($\text{Al}_2\text{O}_3 \cdot 2\text{SiO}_2 \cdot 2\text{H}_2\text{O}$), composed by two molecules of water, losses that water turning into amorphous

silicate ($\text{Al}_2\text{O}_3 \cdot 2\text{SiO}_2$) due to structural collapse [194]. The optimal factors for the thermal treatment are optimizing energy consumption, ensuring maintenance of the amorphous phases, thus reducing crystalline phases formation [191]. Artificial pozzolans can also come directly from industrial wastes, such as fly ash collected in coal thermal plants, rice husk ashes or red ceramic dust, that has not been fired at too high temperatures for too long to avoid/reduce crystalline phase formation [195] (Fig. 5). Nowadays, mainly due to environmental concerns, also other wastes are being studied to be used as pozzolans for lime composites, such as sewage sludge ash or mining wastes [196–198]. In some of those cases, depending on the application of the mortars (namely if as renders or plasters), non-toxic lixiviates and odors must be ensured. Different pozzolans and treatments present very distinct reactivity. Therefore, a lot of research still needs to be done concerning pozzolans.

5.1 Air lime-pozzolan reaction in mortars

Pozzolanic materials react with $\text{Ca}(\text{OH})_2$ of lime-based mortars in the presence of water to produce mainly C–A–H and C–S–H. At the alkaline pH of a calcium hydroxide solution, the high concentration of hydroxyl anions are responsible for the breakage of bonds in SiO_2 , silicates and aluminosilicates, giving rise to ions such as $[\text{SiO}(\text{OH})_3]^-$ and $[\text{Al}(\text{OH})_4]^-$ [199]. In contact with Ca^{2+} ions, these silicate and aluminate ions form hydrated silicates of C–S–H type, calcium aluminate C_4AH_{13} , hydrated gehlenite C_2ASH_8 , and $\text{C}_3\text{A} \cdot \text{CaCO}_3 \cdot 12\text{H}_2\text{O}$. It is interesting to consider that the silicate compounds dissolve more rapidly than aluminate and a higher concentration of calcium ions is required for the formation of the aluminate-based components. Therefore, C–S–H gels precipitate onto the particles of pozzolans firstly [199]. These compounds provide hydraulic performance to the air lime composites. The C–S–H and C–A–H hydrates are similar to the ones formed in mortars with hydraulic binders, namely cement, but the content and type of C–S–H of air lime-pozzolan systems are different. Therefore, contrary to cement mortars, the lime-pozzolanic mortars contribute to physico-chemical compatibility with the mortars of the historic structures [200]. Pozzolans can be used as an addition to the binder but in fact they can partially replace it in mortars formulations [201].



Pozzolanic reactivity can be assessed by the $\text{Ca}(\text{OH})_2$ consumed and the kinetics of the reaction [199]. Different methods can be used to evaluate that pozzolan reactivity [202, 203] but one of the most common is the modified Chapelle test based on a French standard [204] for metakaolin but that is also applied to test other pozzolans. The strength development of lime-pozzolan system can be also monitored by following ASTM C593-19 [205].

The pozzolanic reaction is not fast in comparison to a common hydraulic binder hydration reaction and, in lime mortars, it competes with carbonation, that is an even slower reaction. Lime-pozzolan mortars take about two days to harden but the properties go on developing mainly during the first two–three months. However, it seems that the pozzolanic reaction, at least for some mortar mix designs at ambient temperature and CO_2 content, does not reduce carbonation [109]. Nowadays, other materials are studied in blended mixes to improve air lime-pozzolan mortars performance, such as ternary systems (lime-pozzolana-cement) or nano materials [67, 206, 207].

5.2 Main factors influencing air lime-pozzolan mortars performance

More than 2000 years ago [208], air lime-based and pozzolans composites were used allowing the hardening not only by carbonation but also by hydration. The possibility of lime-based mortars application is thus enlarged even when a weak contact with CO_2 is provided, such as underwater or in deep applications, and increased durability, namely when a frequent contact with water and salts was present.

Adequate water/binder (w/b) ratio and optimized early curing conditions are fundamental to ensure low porosity and, therefore, air lime-pozzolan mortars durability [42]. The w/b should be enough to ensure workability for the application and is strongly influenced by the type of pozzolan and mainly by its specific surface area [191]. Nevertheless, the initial curing must be humid to provide enough moisture for pozzolanic reaction to occur, and to ensure CO_2 transport and further carbonation reaction. If the curing is too dry, the pozzolanic reaction cannot occur due to lack of water for hydrated products formation and the carbonation will be even slower because of slow CO_2 dissolution.

However, the parameters influencing the performance and durability of lime-pozzolan mortars are vast and also include the reactivity of both lime and pozzolan, their proportions on the mortars formulation [66, 201, 209] but also the mortars application technology [8]. The reactivity of the pozzolan will be critical to establish the performance along time [210], giving rise to the different composition and microstructure of the hardened products, as reported by some authors [152, 199, 209]. The percentage of the pozzolanic additive is also important, since a too large amount of the additive may lead to an excessive drying shrinkage [211]. For a more accurate assessment, air lime-pozzolan mortar performance should not only be assessed in laboratory conditions but also in situ [212] and in the literature it seems there is a lack of register of long-term monitoring.

6 Competition between different processes

During the hardening of (a) air lime, (b) NHL, (c) lime-pozzolan and (d) NHL-pozzolan mortars, competitive reactions such as drying, carbonation, hydration and pozzolanic reaction occur. The addition of pozzolanic material, natural or artificial, in hydraulic lime mortars [213] relies on a mechanism similar to that observed in cement mortars or concrete enriched with pozzolans. It was observed that the non-carbonated lime can further react with pozzolans to produce hydraulic components imparting more strength to the final mortar and especially better resistance to sulfates. Generally, in NHL mortars, hydration precedes carbonation, except for pozzolanic materials with low reactivity with lime that favoured the consumption of lime by carbonation reaction. However, moisture greatly influences the degree and the order of these reactions, being hydration mostly enhanced under higher moist conditions and carbonation involved under drier conditions. Remarkable consequences in the mechanical properties impose that NHL and lime-pozzolan mortars should be cured in moist conditions for promoting the early hydration. Other parameters involved in the competition of processes are the quantity of calcium hydroxide affecting the carbonation along with the quantity of calcium silicates and aluminates influencing the physical and mechanical properties.

6.1 Drying versus carbonation

Oliveira et al. [214] addressed an experimental program for elucidating the competition between drying process and evolution of carbonation in air lime mortars. In air lime mortars the humidity diffusion was quicker than the one normally observed in cement-based materials [214]. Drying process has been observed in air lime mortars, before carbonation had taken place, resulting in eventual drying shrinkage and subsequent surface cracks [215].

Carbonation is influenced by the surrounding environment and characteristics of the material. The characteristics of the porous matrix affect the depth of the carbonation front [216, 217] and full carbonation may take decades or even centuries in thick elements [218].

In general, the evolution of mechanical properties of air lime mortars are related to drying and carbonation processes, which are in turn coupled together [214]. Water vapour enables the reaction between CO_2 and calcium hydroxide leading to the hardening of air mortars, establishing those surfaces as net CO_2 uptake.

Based on the literature review by Despotou et al. [99], the mechanisms and kinetics of carbonation depend strongly on the mineralogy, texture of mortars, type of additive and lime used, the width of the walls, thickness of the mortar (less carbonation when mortar depth increases), as well as the timeframe allowing the carbonation process to take place. Under natural conditions, actual building practice and depending on the thickness of the mortar/plaster, carbonation takes between a few weeks and several years (see also discussion in Sect. 3.4).

6.2 Carbonation versus hydration

In this section, the competition between carbonation and hydration mechanisms involves mortars with NHL. Parameters of prime importance that influence the progress of those two mechanisms are the mixing water ratio and the curing conditions [8, 93, 102, 219, 220]. A high water content favours the hydration and retards the carbonation process. A quick carbonation occurs within 40% and 80% RH, and moderate temperature [8, 102, 219]; as opposed to that, hydration of hydraulic binders requires 95%-to 100% of RH, especially in the very first days of casting.

These findings are related to the controlling rate step in the carbonation process (dissolution and diffusion of CO_2). Appropriate RH values induce best dissolution and diffusion processes of CO_2 in pore solution [93], resulting in increasing values of available CO_2 within the system [99]. On the other hand, this water presence allows the calcium hydroxide dissolution and thus its availability for carbonation. The heat release during the calcium carbonate formation in high CO_2 ratios leads to water evaporation, thus decreasing both carbonation and hydration rate [105, 106].

Other factors affecting the competition of the mechanisms include the raw materials nature and quantity, the thickness and place of mortars in the structure, as well as the mortar conservation state that is related to changes in composition and texture [97, 100, 108]. Portlandite was detected in NHL mortars applied to a Venetian villa after 3 years of application and it was attributed to the ongoing hydration reaction and to the humid environment not promoting the carbonation [37].

6.3 Drying and/or hydration versus pozzolanic reaction

The setting and hardening processes of lime-pozzolan mortars are strongly affected by the presence of water. If the pozzolanic material has low reactivity, competition between drying and pozzolanic reaction can take place in lime-pozzolan mortars under atmospheric conditions. Even highly reactive pozzolanic material like metakaolin may not provide enough strength development to the mortar due to phase modifications. The main phases formed in the reaction of lime and metakaolin are the calcium silicate hydrate (C-S-H), the calcium aluminate hydrate, stratlingite (C_2ASH_8), the tetra calcium aluminate hydrate (C_4AH_{13}) and the monocarboaluminate $\text{C}_4\text{AcH}_{11}$ ($3\text{CaO}\cdot\text{Al}_2\text{O}_3\cdot\text{CaCO}_3\cdot 11\text{H}_2\text{O}$). Regarding the stability of these phases, namely the transformation of stratlingite and C_4AH_{13} into hydrogarnet at long term, can result in decrease of the compressive strength [49, 221, 222]. Therefore, the hydrated phases and their stability are crucial for the achievement of sufficient strength.

Due to the gradual progress of the hydration reactions, lime-pozzolan mortars require moist conditions to ensure enough strength development. Curing under dry conditions does not sufficiently increase



their strength because the hydration reactions are slowed down or even terminated by the full carbonation of lime in lime-pozzolan mortars. Therefore, lime-pozzolan mortars should be treated with moist curing during early stages to improve the hydration reactions.

In this category of mortars, the definition of the competition of processes is more complicated as additional and competitive factors influence the hardening of the mortar, such as the effectiveness and content of the pozzolan, the curing conditions, as well as the presence of additives and admixtures in the mortar. Arizzi and Cultrone [209] studied the carbonation process and the pozzolanic reaction of lime-metakaolin (MK) mortars in different wt% addition of MK. As observed, the addition of MK retarded the carbonation in mixtures with addition of 10 and 15% MK, whereas the 20% MK mortars exhibited higher carbonation at early stages, fact that could be related to the formation of more monocarboaluminate phases. Furthermore, compressive strength decreases in 3 months of curing time, due to microcracks formed by the shrinkage that took place over curing [223]. On the contrary, when carbonation preceded the pozzolanic reaction, mechanical properties such as long-term compressive strength and toughness are enhanced, because of the formation of stable monocarboaluminate phases that hindered the hydrogarnet appearance [224].

The occurrence of pozzolanic reaction and hydration in ternary mixes including NHL with pozzolanic additives should be considered as an effective alternative in some cases. NHL binders enriched with pozzolanic material yield compact structures formed by C-S(A)-H and calcite, since pozzolanic reaction in the presence of moist conditions and carbonation occurred continuously [225]. The strength gained by the hydration reaction of NHL can be improved by using pozzolanic material, as the portlandite produced during the hydration process of NHL can be either carbonated and/or reacted with the pozzolanic material to yield newly-formed C-S(A)-H.

It seems reasonable to argue that in those ternary systems moist curing conditions that favour the hydraulic components formation could be recommended as those prevent from the carbonation of free lime and derived portlandite. However, more research is needed to define the mechanisms governing the

short and long-term curing stages of those ternary systems.

7 Conclusions

Drying influences significantly all the mortars characteristics, including microstructure, mechanical and hygric performance and durability. Drying is controlled by the composition of the mortar (binder type, aggregate nature and ratio and mixing water ratio), by curing conditions (temperature, RH, air velocity) and by porous media in contact.

The carbonation of a lime mortar is controlled by the amount of water in the inner part of the mortar (that is, by the RH and by the mixing water ratio), by the aggregate ratio, by the particle size of the portlandite crystals and by the thickness of the masonry (limiting the water evaporation and the CO₂ access). For the carbonation a range of 40–80% of RH would be necessary, being the optimal range from 70–80%.

However, for natural hydraulic lime mortars and for lime-cement mortars, higher RH are suggested. A humid environment allows the hydration of the hydraulic components. The mineralogical composition (the ratio of the hydraulic phases and their composition) and the ratios of mixing water and of aggregate also have a clear influence on the setting and hardening of the hydraulic mortars, which show a sharper development of strength from 0 to 28 days and at long curing periods (from 182 to 365 days). Lime-cement mortars also exhibit a long-term strength development, ascribed to lime carbonation.

Pozzolanic reaction requires a humid environment, so that the factors in connection with the amount of water are of importance. Apart from mineralogical composition, the specific surface of the pozzolans is a critical parameter to explain their reactivity. At least for some mortar mix designs at normal conditions of temperature and CO₂, the pozzolanic reaction does not reduce carbonation.

In air lime mortars, the humidity diffusion (by evaporation or absorption by substrate) takes place before any noticeable carbonation. Providing an adequate humid environment, hydration precedes carbonation, except for pozzolanic materials with low reactivity with lime that favoured the consumption of lime by carbonation reaction. Ternary mixtures including hydraulic limes and pozzolans may result in

the improvement of the performance of the mortars under appropriate curing conditions.

Consequently, for realistic application, testing conditions and studies on these mortars are important, namely: to know the mineralogical composition and the particle size distribution of the binder and additions to be used (ratio of hydraulic components, mineralogical composition, particle size of the lime and pozzolans); to adequately define curing parameters, which must be appropriate for each kind of binder and additions, and also be feasible in practice, as a function of the final purpose of the mortar; to design appropriate mixing ratios (water/binder, binder/aggregate, pozzolanic additions when deemed necessary); and to consider the effect of porous substrates, particularly in the case of air lime mortars.

Compliance with ethical standards

Conflict of interest All co-authors are members in RILEM TC 277-LHS. The authors declare that they have no conflict of interest.

Open Access This article is licensed under a Creative Commons Attribution 4.0 International License, which permits use, sharing, adaptation, distribution and reproduction in any medium or format, as long as you give appropriate credit to the original author(s) and the source, provide a link to the Creative Commons licence, and indicate if changes were made. The images or other third party material in this article are included in the article's Creative Commons licence, unless indicated otherwise in a credit line to the material. If material is not included in the article's Creative Commons licence and your intended use is not permitted by statutory regulation or exceeds the permitted use, you will need to obtain permission directly from the copyright holder. To view a copy of this licence, visit <http://creativecommons.org/licenses/by/4.0/>.

References

1. Elert K, Rodriguez-Navarro C, Sebastian Pardo E et al (2002) Lime mortars for the conservation of historic buildings. *Stud Conserv* 47:62–75. <https://doi.org/10.1179/sic.2002.47.1.62>
2. Lanás J, Alvarez JI (2003) Masonry repair lime-based mortars: Factors affecting the mechanical behavior. *Cem Concr Res* 33:1867–1876. [https://doi.org/10.1016/S0008-8846\(03\)00210-2](https://doi.org/10.1016/S0008-8846(03)00210-2)
3. Stefanidou M, Papayianni I (2005) The role of aggregates on the structure and properties of lime mortars. *Cem Concr Comp* 27:914–919. <https://doi.org/10.1016/j.cemconcomp.2005.05.001>
4. Apostolopoulou M, Delegou ET, Alexaki E et al (2018) Study of the historical mortars of the Holy Aedicule as a basis for the design, application and assessment of repair mortars: a multispectral approach applied on the Holy Aedicule. *Constr Build Mater* 181:618–637. <https://doi.org/10.1016/j.conbuildmat.2018.06.016>
5. Botas S, Veiga R, Velosa A et al (2020) Compatible air lime mortars for historical tiled facades: bond and mechanical strength versus tile-mortar interface microstructure. *J Mater Civ Eng* 32:04020112. [https://doi.org/10.1061/\(ASCE\)MT.1943-5533.0003121](https://doi.org/10.1061/(ASCE)MT.1943-5533.0003121)
6. Sena da Fonseca B, Ferreira Pinto AP, Vaz Silva D (2020) Compositional and textural characterization of historical bedding mortars from rubble stone masonries: contribution for the design of compatible repair mortars. *Constr Build Mater* 247:118627. <https://doi.org/10.1016/j.conbuildmat.2020.118627>
7. Segura J, Aponte D, Pela L et al (2020) Influence of recycled limestone filler additions on the mechanical behaviour of commercial premixed hydraulic lime based mortars. *Constr Build Mater* 238:117722. <https://doi.org/10.1016/j.conbuildmat.2019.117722>
8. Veiga R (2017) Air lime mortars: What else do we need to know to apply them in conservation and rehabilitation interventions? A review. *Constr Build Mater* 157:132–140. <https://doi.org/10.1016/j.conbuildmat.2017.09.080>
9. Schlegel T, Shtiza A (2016) Lime carbonation, environmental footprint of seven mortars placed on the European market. In: *Brick and Block Masonry: Trends, Innovations and Challenges—Proceedings of the 16th international brick and block masonry conference, IBMAC 2016. 16th international brick and block masonry conference, IBMAC 2016; Padova; Italy; 26 June 2016 through 30 June 2016; Code 176009, pp 931–936*
10. Forster AM, Válek J, Hughes JJ et al (2020) Lime binders for the repair of historic buildings: considerations for CO₂ abatement. *J Clean Prod* 252:119802. <https://doi.org/10.1016/j.jclepro.2019.119802>
11. Bras A, Faria P (2017) Effectiveness of mortars composition on the embodied carbon long-term impact. *Energy Build* 154:523–528. <https://doi.org/10.1016/j.enbuild.2017.08.026>
12. Hughes JJ et al (2012) (2012) RILEM TC 203-RHM: repair mortars for historic masonry. *Mater Struct* 45:1287–1294. <https://doi.org/10.1617/s11527-012-9847-9>
13. Stefanidou M, Pachta V, Konopissi S et al (2014) Analysis and characterization of hydraulic mortars from ancient cisterns and baths in Greece. *Mater Struct* 47:571–580. <https://doi.org/10.1617/s11527-013-0080-y>
14. Nunes C, Pel L, Kunecky J et al (2017) The influence of the pore structure on the moisture transport in lime plaster-brick systems as studied by NMR. *Constr Build Mater* 142:395–409. <https://doi.org/10.1016/j.conbuildmat.2017.03.086>
15. Nogueira R, Ferreira Pinto AP et al (2018) Design and behavior of traditional lime-based plasters and renders. Review and critical appraisal of strengths and weaknesses. *Cem Concr Comp* 89:192–204. <https://doi.org/10.1016/j.cemconcomp.2018.03.005>
16. Vyšvařil M, Pavlíková M, Záleská M et al (2020) Non-hydrophobized perlite renders for repair and thermal insulation purposes: Influence of different binders on their



- properties and durability. *Constr Build Mater* 263:120617. <https://doi.org/10.1016/j.conbuildmat.2020.120617>
17. Vavricuk A, Bokan-Bosiljkov V, Kramar S (2018) The influence of metakaolin on the properties of natural hydraulic lime-based grouts for historic masonry repair. *Constr Build Mater* 172:706–716. <https://doi.org/10.1016/j.conbuildmat.2018.04.007>
 18. Luso E, Lourenco PB (2017) Experimental laboratory design of lime based grouts for masonry consolidation. *Int J Archit Herit* 11:1143–1152. <https://doi.org/10.1080/15583058.2017.1354095>
 19. González-Sánchez JF, Taşçı B, Fernández JM et al (2020) Combination of polymeric superplasticizers, water repellents and pozzolanic agents to improve air lime-based grouts for historic masonry repair. *Polymers* 12:887–912. <https://doi.org/10.3390/polym12040887>
 20. Dinç-Şengönül B, Oktay D, Yüzer N (2020) Effect of temperature, resting time and brick dust (Horasan) on the rheological properties of hydraulic lime-based grouts. *Constr Build Mater* 265:120644
 21. Pachta V, Goulas D (2020) Fresh and hardened state properties of fiber reinforced lime-based grouts. *Constr Build Mater* 261:119818. <https://doi.org/10.1016/j.conbuildmat.2020.119818>
 22. Duran A, Robador MD, Jimenez de Haro MC et al (2010) Seville City Hall Chapter Room ceiling decoration. *Mater Constr* 60:83–95. <https://doi.org/10.3989/mc.2010.45107>
 23. Ma X, Wei G, Grifa C et al (2018) Multi-analytical studies of archaeological Chinese earthen plasters: the inner wall of the Longhu Hall (Yuzhen Palace, Ancient Building Complex, Wudang Mountains, China). *Archaeometry* 60:1–18. <https://doi.org/10.1111/arc.12318>
 24. Pecchioni E, Malesani P, Bellucci B et al (2005) Artificial stones utilised in Florence historical palaces between the XIX and XX centuries. *J Cult Herit* 6:227–233. <https://doi.org/10.1016/j.culher.2005.06.001>
 25. Girginova P, Galacho C, Veiga MR et al (2020) Study of mechanical properties of alkaline earth hydroxide nanoconsolidants for lime mortars. *Constr Build Mater* 236:117520. <https://doi.org/10.1016/j.conbuildmat.2019.117520>
 26. Mateos L, Esquivel D, Cosano D et al (2018) Micro-Raman analysis of mortars and wallpaintings in the Roman villa of Fuente Alamo (Puente Genil, Spain) and identification of the application technique. *Sens Actuators A Phys* 281:15–23. <https://doi.org/10.1016/j.sna.2018.08.038>
 27. Jerónimo A, Camões A, Aguiar JL et al (2019) Hydraulic lime mortars with antifungal properties. *Appl Surf Sci* 483:1192–1198. <https://doi.org/10.1016/j.apsusc.2019.03.156>
 28. Válek J, Hughes JJ, Pique F, Gulotta D, van Hees R, Papayiani I (2019) Recommendation of RILEM TC 243-SGM: functional requirements for surface repair mortars for historic buildings. *Mater Struct* 52:28. <https://doi.org/10.1617/s11527-018-1284-y>
 29. Pachta V, Marinou P, Stefanidou M (2018) Development and testing of repair mortars for floor mosaic substrates. *J Build Eng* 20:501–509. <https://doi.org/10.1016/j.job.2018.08.019>
 30. Felekoğlu B, Gödek E, Ersoy A et al (2016) Physical, mechanical and microstructural characterization of basilica plasters and bouleterion mortars in smyrna agora. *Mediterr Archaeol Archaeom* 16:193–202. <https://doi.org/10.5281/zenodo.35532>
 31. Martínez García C, Fonteboa B, Diego C et al (2019) Impact of mussel shell aggregates on air lime mortars. Pore structure and carbonation. *J Clean Prod* 215:650–668. <https://doi.org/10.1016/j.jclepro.2019.01.121>
 32. Arizzi A, Cultrone G (2014) The water transfer properties and drying shrinkage of aerial lime based mortars: an assessment of their quality as repair rendering materials. *Environ Earth Sci* 71:1699–1710. <https://doi.org/10.1007/s12665-013-2574-x>
 33. Lanás J, Pérez Bernal JL, Bello MA et al (2006) Mechanical properties of masonry repair dolomitic lime-based mortars. *Cem Concr Res* 36:951–960. <https://doi.org/10.1016/j.cemconres.2005.10.004>
 34. Arizzi A, Cultrone G (2012) The difference in behaviour between calcitic and dolomitic lime mortars set under dry conditions: The relationship between textural and physical-mechanical properties. *Cem Concr Res* 42:818–826. <https://doi.org/10.1016/j.cemconres.2012.03.008>
 35. Chever L, Pavia S, Howard R (2010) Physical properties of magnesian lime mortars. *Mat Struct* 43:283–296. <https://doi.org/10.1617/s11527-009-9488-9>
 36. Schork J (2012) Dolomitic lime in the US history, development and physical characteristics. *J Archit Conserv* 18:7–25. <https://doi.org/10.1080/13556207.2012.10785116>
 37. Maravelaki-Kalaitzaki P, Bakolas A, Karatasios I et al (2005) Hydraulic lime mortars for the restoration of historic masonry in Crete. *Cem Concr Res* 35:1577–1586. <https://doi.org/10.1016/j.cemconres.2004.09.001>
 38. Baltazar LG, Henriques FMA, Jorne F et al (2014) Combined effect of superplasticizer, silica fume and temperature in the performance of natural hydraulic lime grouts. *Constr Build Mater* 50:584–597. <https://doi.org/10.1016/j.conbuildmat.2013.10.005>
 39. Lanás J, Perez Bernal JL, Bello MA et al (2004) Mechanical properties of natural hydraulic lime-based mortars. *Cem Concr Res* 34:2191–2201. <https://doi.org/10.1016/j.cemconres.2004.02.005>
 40. EN 459-1 (2015) Building lime—part 1: definitions, specifications and conformity criteria
 41. Grilo J, Santos Silva A, Faria P et al (2014) Mechanical and mineralogical properties of natural hydraulic lime-metakaolin mortars in different curing conditions. *Constr Build Mater* 51:287–294. <https://doi.org/10.1016/j.conbuildmat.2013.10.045>
 42. Papayianni I, Stefanidou M (2006) Strength–porosity relationships in lime–pozzolan mortars. *Constr Build Mater* 20:700–705. <https://doi.org/10.1016/j.conbuildmat.2005.02.012>
 43. Matias G, Faria P, Torres I (2014) Lime mortars with ceramic wastes: characterization of components and their influence on the mechanical behaviour. *Constr Build Mater* 73:523–534. <https://doi.org/10.1016/j.conbuildmat.2014.09.108>
 44. Ferraz E, Andrejkovičová S, Velosa A et al (2014) Synthetic zeolite pellets incorporated to air lime–metakaolin mortars: Mechanical properties. *Constr Build Mater*



- 69:243–252. <https://doi.org/10.1016/j.conbuildmat.2014.07.030>
45. Stefanidou M (2016) Use of natural pozzolans with lime for producing repair mortars. *Environ Earth Sci* 75:758. <https://doi.org/10.1007/s12665-016-5444-5>
 46. Pineda P, Garcia-Martinez A, Castizo-Morales D (2017) Environmental and structural analysis of cement-based vs. natural material-based grouting mortars. Results from the assessment of strengthening works. *Constr Build Mater* 138:528–547. <https://doi.org/10.1016/j.conbuildmat.2017.02.013>
 47. Cizer O, Van Balen K, Van Gemert D, Elsen J (2008) Blended lime–cement mortars for conservation purposes: microstructure and strength development. In: D’Ayala, Fodde (eds) SAHC08, pp 965–972
 48. Arandigoyen M, Alvarez JI (2007) Pore structure and mechanical properties of cement-lime mortars. *Cem Concr Res* 37:767–775. <https://doi.org/10.1016/j.cemconres.2007.02.023>
 49. Sepulcre-Aguilar A, Hernandez-Olivares F (2010) Assessment of phase formation in lime-based mortars with added metakaolin, Portland cement and sepiolite, for grouting of historic masonry. *Cem Concr Res* 40:66–76. <https://doi.org/10.1016/j.cemconres.2009.08.028>
 50. Silva BA, Ferreira Pinto AP, Gomes A (2015) Natural hydraulic lime versus cement for blended lime mortars for restoration works. *Constr Build Mater* 94:346–360. <https://doi.org/10.1016/j.conbuildmat.2015.06.058>
 51. Ramesh M, Azenha M, Lourenco PB (2019) Quantification of impact of lime on mechanical behaviour of lime cement blended mortars for bedding joints in masonry systems. *Constr Build Mater* 229:116884. <https://doi.org/10.1016/j.conbuildmat.2019.116884>
 52. Válek J, Skružná O, Kozlovcev P et al (2020) Composition and technology of the 17th century stucco decorations at Červená Lhota Castle in Southern Bohemia. *Int J Archit Herit* 14:1042–1057. <https://doi.org/10.1080/15583058.2020.1731627>
 53. Charola AE, Henriques FMA (1999) Lime mortars: some considerations on testing standardization. Use of and need for preservation standards in architectural conservation: American Society for Testing and Materials Special Technical Publications 1355, pp 142–151
 54. Pachta V, Gulotta D, Valek J, Papayianni I (2019) Evaluation of the fresh state properties of lime-based grouts through inter-laboratory comparative testing. In: Álvarez JI, Fernández JM, Navarro I, Durán A, Sirera R (eds) 5th historic mortars conference, pp 1225–1237
 55. Pachta V, Papayianni I, Spyriiotis T (2020) Assessment of laboratory and field testing methods in lime-based grouts for the consolidation of architectural surfaces. *Int J Archit Herit*. <https://doi.org/10.1080/15583058.2020.1731629>
 56. Izaguirre A, Lanás J, Alvarez JI (2010) Behaviour of a starch as a viscosity modifier for aerial lime-based mortars. *Carbohydr Polym* 80:222–228. <https://doi.org/10.1016/j.carbpol.2009.11.010>
 57. Izaguirre A, Lanás J, Alvarez JI (2011) Characterization of aerial lime-based mortars modified by the addition of two different water-retaining agents. *Cem Concr Comp* 33:309–318. <https://doi.org/10.1016/j.cemconcomp.2010.09.008>
 58. Pavia S, Aly M (2016) Influence of aggregate and supplementary cementitious materials on the properties of hydrated lime (CL90s) mortars. *Mater Constr* 66:e104. <https://doi.org/10.3989/mc.2016.01716>
 59. Winnefeld F, Böttger KG (2006) How clayey fines in aggregates influence the properties of lime mortars. *Mater Struct* 39:433–443. <https://doi.org/10.1617/s11527-005-9023-6>
 60. Pozo-Antonio JS (2015) Evolution of mechanical properties and drying shrinkage in lime-based and lime cement-based mortars with pure limestone aggregate. *Constr Build Mater* 77:472–478. <https://doi.org/10.1016/j.conbuildmat.2014.12.115>
 61. Drougkas A, Roca P, Molins C (2016) Compressive strength and elasticity of pure lime mortar masonry. *Mater Struct* 49:983–999. <https://doi.org/10.1617/s11527-015-0553-2>
 62. Lawrence M, Mays T, Rigby S et al (2007) Effects of carbonation on the pore structure of non-hydraulic lime mortars. *Cem Concr Res* 37:1059–1069. <https://doi.org/10.1016/j.cemconres.2007.04.011>
 63. Santos AR, Veiga MR, Santos Silva A et al (2018) Evolution of the microstructure of lime based mortars and influence on the mechanical behaviour: the role of the aggregates. *Constr Build Mater* 187:907–922. <https://doi.org/10.1016/j.conbuildmat.2014.12.115>
 64. Izaguirre A, Lanás J, Alvarez JI (2010) Ageing of lime mortars with admixtures: durability and strength assessment. *Cem Concr Res* 40:1081–1095. <https://doi.org/10.1016/j.cemconres.2010.02.013>
 65. Lanás J, Sirera R, Alvarez JI (2006) Study of the mechanical behaviour of masonry repair lime-based mortars cured and exposed under different conditions. *Cem Concr Res* 36:961–970. <https://doi.org/10.1016/j.cemconres.2005.12.003>
 66. Arizzi A, Viles H, Cultrone G (2012) Experimental testing of the durability of lime-based mortars used for rendering historic buildings. *Constr Build Mater* 28:807–818. <https://doi.org/10.1016/j.conbuildmat.2011.10.059>
 67. Duran A, Navarro-Blasco I, Fernández JM et al (2014) Long-term mechanical resistance and durability of air lime mortars with large additions of nanosilica. *Constr Build Mater* 58:147–158. <https://doi.org/10.1016/j.conbuildmat.2014.02.030>
 68. El-Turki A, Ball R, Holmes S et al (2010) Environmental cycling and laboratory testing to evaluate the significance of moisture control for lime mortars. *Constr Build Mater* 24:1392–1397. <https://doi.org/10.1016/j.conbuildmat.2010.01.019>
 69. Nunes C, Slizkova Z (2014) Hydrophobic lime based mortars with linseed oil: Characterization and durability assessment. *Cem Concr Res* 61–62:28–39. <https://doi.org/10.1016/j.cemconres.2014.03.011>
 70. Torres I, Veiga R, Freitas V (2018) Influence of substrate characteristics on behavior of applied mortar. *J Mater Civ Eng* 30:04018254. [https://doi.org/10.1061/\(ASCE\)MT.1943-5533.0002339](https://doi.org/10.1061/(ASCE)MT.1943-5533.0002339)
 71. Gameiro A, Santos Silva A, Veiga R et al (2013) Phase and microstructural characterization of Lime-MK blended mixes. In: Pinto AMP, Pouzada AS (eds) Materials science



- forum, pp 135–140. <https://doi.org/10.4028/www.scientific.net/MSF.730-732.135>
72. Santos Silva A, Gameiro A, Grilo J et al (2014) Long-term behavior of lime–metakaolin pastes at ambient temperature. *Appl Clay Sci* 88–89:49–55. <https://doi.org/10.1016/j.clay.2013.12.016>
 73. Papayianni I (1999) Parameters affecting the performance of lime based repair mortars. In: *Materials science and restoration MSRV*, vol 2. AEDIFICATIO Publishers, pp 1329–1337
 74. Pavlík V, Užáková M (2016) Effect of curing conditions on the properties of lime, lime–metakaolin and lime–zeolite mortars. *Constr Build Mater* 102:14–25. <https://doi.org/10.1016/j.conbuildmat.2015.10.128>
 75. Rodriguez-Navarro C, Ruiz-Agudo E (2018) Nanolimes: from synthesis to application. *Pure Appl Chem* 90:523–550. <https://doi.org/10.1515/pac-2017-0506>
 76. Veiga R (2000) Influence of application conditions on the cracking susceptibility of renderings. RILEM Publications S.A.:R.L. *Concr Sci Eng* 2:134–140
 77. Eiras JN, Popovics JS, Borrachero MV et al (2015) The effects of moisture and micro-structural modifications in drying mortars on vibration-based NDT methods. *Constr Build Mater* 94:565–571. <https://doi.org/10.1016/j.conbuildmat.2015.07.078>
 78. Scherer GW (1990) Theory of Drying. *J Am Ceram Soc* 73:3–14. <https://doi.org/10.1111/j.1151-2916.1990.tb05082.x>
 79. Arandigoyen M, Alvarez JI (2006) Blended pastes of cement and lime: Pore structure and capillary porosity. *Appl Surf Sci* 252:8077–8085. <https://doi.org/10.1016/j.apsusc.2005.10.019>
 80. Groot C (1993) Effects of water on mortars-brick bond. Dissertation. Delft University of Technology
 81. Botas S, Veiga M, Velosa A (2015) Adhesion of air lime-based mortars to old tiles: moisture and open porosity influence in tile/mortar interfaces. *J Mater Civ Eng* 27:04014161. [https://doi.org/10.1061/\(ASCE\)MT.1943-5533.0001108](https://doi.org/10.1061/(ASCE)MT.1943-5533.0001108)
 82. Válek J, Skružná O (2019) Performance assessment of custom-made replications of an original historic render—a study of application influences. *Constr Build Mater* 229:116822. <https://doi.org/10.1016/j.conbuildmat.2019.116822>
 83. Kanna V, Olson RA, Jennings HM (1998) Effect of shrinkage and moisture content on the physical characteristics of blended cement mortars. *Cem Concr Res* 28:1467–1477. [https://doi.org/10.1016/S0008-8846\(98\)00120-3](https://doi.org/10.1016/S0008-8846(98)00120-3)
 84. Moukwa M, Aitcin PC (1988) The effect of drying on cement pastes pore structure as determined by mercury porosimetry. *Cem Concr Res* 18:745–752. [https://doi.org/10.1016/0008-8846\(88\)90098-1](https://doi.org/10.1016/0008-8846(88)90098-1)
 85. López-Arce P, Gómez-Villalba LS, Martínez-Ramírez S et al (2011) Influence of relative humidity on the carbonation of calcium hydroxide nanoparticles and the formation of calcium carbonate polymorphs. *Powder Technol* 205:263–269. <https://doi.org/10.1016/j.powtec.2010.09.026>
 86. Rodriguez-Navarro C, Elert K, Ševčík R (2016) Amorphous and crystalline calcium carbonate phases during carbonation of nanolimes: implications in heritage conservation. *Cryst Eng Comm* 18:6594–6607. <https://doi.org/10.1039/C6CE01202G>
 87. Martínez-Ramírez S, Sánchez-Cortés S, García-Ramos JV et al (2003) Micro-Raman spectroscopy applied to depth profiles of carbonates formed in lime mortar. *Cem Concr Res* 33:2063–2068. [https://doi.org/10.1016/S0008-8846\(03\)00227-8](https://doi.org/10.1016/S0008-8846(03)00227-8)
 88. Veiga R, Abrantes V (1998) Improving the cracking resistance of rendering mortars. Influence of composition factors. *Int J Housing Sci* 22:245–254
 89. Mauroux T, Benboudjema F, Turcry P et al (2012) Study of cracking due to drying in coating mortars by digital image correlation. *Cem Concr Res* 42:1014–1023. <https://doi.org/10.1016/j.cemconres.2012.04.002>
 90. Faria P, Martins A (2013) Influence of lime type and curing conditions on lime and lime–metakaolin mortars. In: de Freitas VP, Delgado JMPQ (eds) *Durability of building materials and components, building pathology and rehabilitation*, vol 3, VIII. Springer, Berlin, pp 105–126. https://doi.org/10.1007/978-3-642-37475-3_5
 91. Moorehead DR (1986) Cementation by the carbonation of hydrated lime. *Cem Concr Res* 16:700–708. [https://doi.org/10.1016/0008-8846\(86\)90044-X](https://doi.org/10.1016/0008-8846(86)90044-X)
 92. Lawrence R (2006) A Study of carbonation in nonhydraulic lime mortars. Dissertation, University of Bath
 93. Cizer O (2016) Lime mortars in heritage: fundamental insights into carbonation reaction and its biocatalization. In: Van Balen K, Verstrynghe E (eds) *Structural analysis of historical constructions: anamnesis, diagnosis, therapy, controls*, pp 67–74
 94. Cizer Ö, Van Balen K, Elsen J et al (2012) Real-time investigation of reaction rate and mineral phase modifications of lime carbonation. *Constr Build Mater* 35:741–751. <https://doi.org/10.1016/j.conbuildmat.2012.04.036>
 95. Van Balen K (1991) *Karbonatatie van kalkmortel en haar invloed op historische structuren (Carbonation of lime mortars and its influence on historical structures)*. Dissertation, Katholieke Universiteit Leuven
 96. Beruto DT, Botter R (2000) Liquid-like H₂O adsorption layers to catalyze the Ca(OH)₂/CO₂ solid-gas reaction and to form a non-protective solid product layer at 20 °C. *J Eu Ceram Soc* 20:497–503
 97. Ferreti D, Bazant ZP (2006) Stability of ancient masonry towers: moisture diffusion, carbonation and size effect. *Cem Concr Res* 36:1379–1388. <https://doi.org/10.1016/j.cemconres.2006.03.013>
 98. Arandigoyen M, Álvarez JI (2006) Carbonation process in lime pastes with different water/binder ratio. *Mater Constr* 56:5–18. <https://doi.org/10.3989/mc.2016.01716>
 99. Despotou E, Shtiza A, Schlegel T et al (2016) Literature study on the rate and mechanism of carbonation of lime in mortars/Literaturstudie über Mechanismus und Grad der Karbonatisierung von Kalkhydrat im Mörtel. *Mauerwerk* 20:124–137. <https://doi.org/10.1002/dama.201500674>
 100. Lawrence RMH, Mays TJ, Walker P et al (2006) Determination of carbonation profiles in non-hydraulic lime mortars using thermogravimetric analysis. *Thermochim Acta* 444:179–189. <https://doi.org/10.1016/j.tca.2006.03.002>



101. Camerini R, Poggi G, Chelazzi D et al (2019) The carbonation kinetics of calcium hydroxide nanoparticles: a boundary nucleation and growth description. *J Colloid Interface Sci* 547:370–381
102. Van Balen K, Van Gemert D (1994) Modelling lime mortar carbonation. *Mater Struct* 27:393–398. <https://doi.org/10.1007/BF02473442>
103. Cizer O, Van, Elsen J, Van Gemert D (2008) Carbonation reaction kinetics of lime binders measured using XRD. In: Bacciocchi R, Costa G, Poletini A, Pomi R (eds) Conference on accelerated carbonation for environmental and materials engineering, pp 139–148
104. Carcasses M, Petit JY, Ollivier JP (1998) Gas permeability of mortars in relation to the microstructure of interfacial transition zone. In: Katz A, Bentur A, Alexander M, Arliguie G (eds) Second international conference on the interfacial transition zone in cementitious composites, pp 85–92
105. Cultrone G, Sebastian E, Ortega Huertas M (2005) Forced and natural carbonation of lime-based mortars with and without additives: Mineralogical and textural changes. *Cem Concr Res* 35:2278–2289. <https://doi.org/10.1016/j.cemconres.2004.12.012>
106. Van Balen K (2005) Carbonation reaction of lime, kinetics at ambient temperature. *Cem Concr Res* 35:647–657. <https://doi.org/10.1016/j.cemconres.2004.06.020>
107. Dheilly RM, Tudo J, Sebaibi Y et al (2002) Influence of storage conditions on the carbonation of powdered Ca(OH)₂. *Constr Build Mater* 16:155–161. [https://doi.org/10.1016/S0950-0618\(02\)00012-0](https://doi.org/10.1016/S0950-0618(02)00012-0)
108. Dheilly RM, Tudo J, Quénedec M (1998) Influence of climatic conditions on the carbonation of quicklime. *J Mater Eng Perform* 7:789–795. <https://doi.org/10.1361/105994998770347378>
109. Ergenç D, Fort R (2018) Accelerating carbonation in lime-based mortar in high CO₂ environments. *Constr Build Mater* 188:314–325. <https://doi.org/10.1016/j.conbuildmat.2018.08.125>
110. Rodriguez-Navarro C, Hansen E, Ginell WS (1998) Calcium hydroxide crystal evolution upon aging of lime putty. *J Am Ceram Soc* 81(11):3032–3034. <https://doi.org/10.1111/j.1151-2916.1998.tb02735.x>
111. Cazalla O, Rodriguez-Navarro C, Sebastian E et al (2000) Ageing of lime putty: Effects on traditional lime mortar carbonation. *J Am Ceram Soc* 83:1071–1076. <https://doi.org/10.1111/j.1151-2916.2000.tb01332.x>
112. Margalha MG, Silva AS, Do Rosário Veiga M et al (2013) Microstructural changes of lime putty during aging. *J Mater Civ Eng* 25:1524–1532. [https://doi.org/10.1061/\(ASCE\)MT.1943-5533.0000687](https://doi.org/10.1061/(ASCE)MT.1943-5533.0000687)
113. Moropoulou A, Bakolas A, Aggelakopoulou E (2001) The effects of limestone characteristics and calcination temperature to the reactivity of the quicklime. *Cem Concr Res* 31:633–639. [https://doi.org/10.1016/S0008-8846\(00\)00490-7](https://doi.org/10.1016/S0008-8846(00)00490-7)
114. Rodriguez-Navarro C, Ruiz-Agudo E, Luque A et al (2009) Thermal decomposition of calcite: mechanisms of formation and textural evolution of CaO nanocrystals. *Am Miner* 94:578–593. <https://doi.org/10.2138/am.2009.3021>
115. Kingery WD (1960) Introduction to ceramics. Wiley, New York
116. McClellan GH, Eades JL (1970) The textural evolution of limestone calcines. In: The reaction parameters of lime, ASTM special publication 472. American Society for Testing and Materials, Philadelphia, pp 209–227
117. Sala E, Giustina I, Plizzari GA (2008) Lime mortar with natural pozzolana: Historical issues and mechanical behavior. In: D' Ayala, Fodde (eds) Structural analysis of historic construction. Taylor and Francis Group, London, ISBN 978-0-415-46872-5
118. Ostwald W (1900) Über die vermeintliche Isomerie des roten und gelben Quecksilberoxyds und die Oberflächenspannung fester Körper. *Z Phys Chem* 34:495–503. <https://doi.org/10.1515/zpch-1900-3431>
119. Hansen E, Rodríguez-Navarro C, Van Balen K (2008) Lime putties and mortars. *Stud Conserv* 53:9–23. <https://doi.org/10.1179/sic.2008.53.1.9>
120. Ruiz-Agudo E, Rodríguez-Navarro C (2010) Microstructure and rheology of lime putty. *Langmuir* 26:3868–3877. <https://doi.org/10.1021/la903430z>
121. Bohac M, Necas R (2016) The role of aging on rheological properties of lime putty. *Procedia Eng* 151:34–41. <https://doi.org/10.1016/j.proeng.2016.07.355>
122. Stern KH (1954) The Liesegang phenomenon. *Chem Rev* 54:79–99. <https://doi.org/10.1021/cr60167a003>
123. Rodriguez-Navarro C, Cazalla O, Elert K et al (2002) Liesegang pattern development in carbonating traditional lime mortars. *Proc Math Phys Eng Sci* 458(2025):2261–2273. <https://doi.org/10.1098/rspa.2002.0975>
124. Moropoulou A, Bakolas A, Bisbikou K (1995) Characterization of ancient, byzantine and later historic mortars by thermal and X-ray diffraction techniques. *Thermochim Acta* 269–270:779–795. [https://doi.org/10.1016/0040-6031\(95\)02571-5](https://doi.org/10.1016/0040-6031(95)02571-5)
125. Franzini M, Leoni L, Lezzerini M (2000) A procedure for determining the chemical composition of binder and aggregate in ancient mortars: its application to mortars from some medieval buildings in Pisa. *J Cult Herit* 1:365–373. [https://doi.org/10.1016/S1296-2074\(00\)01092-X](https://doi.org/10.1016/S1296-2074(00)01092-X)
126. Güleç A, Tulun T (1997) Physico-chemical and petrographical studies of old mortars and plasters of Anatolia. *Cem Concr Res* 27:227–234. [https://doi.org/10.1016/S0008-8846\(97\)00005-7](https://doi.org/10.1016/S0008-8846(97)00005-7)
127. Cardiano P, Sergi S, De Stefano C et al (2008) Investigations on ancient mortars from the Basilian monastery of Fragalà. *J Therm Anal Calorim* 91:477–485. <https://doi.org/10.1007/s10973-006-8313-8>
128. Arizzi A, Hendrickx R, Cultrone G, Van Balen K (2012) Differences in the rheological properties of calcitic and dolomitic lime slurries: influence of particle characteristics and practical implications in lime-based mortar manufacturing. *Mater Constr* 62:231–250. <https://doi.org/10.3989/mc.2011.00311>
129. Vyšvařil M, Žižlavský T, Bayer P (2017) Influence of the aggregate type on the properties of dolomitic lime-based mortars. *Key Eng Mat* 722:343–350
130. Dheilly RM, Bouguerra A, Beaudoin B et al (1999) Hydromagnesite development in magnesian lime mortars. *Mater Sci Eng A* 268:127–131. [https://doi.org/10.1016/S0921-5093\(99\)00085-4](https://doi.org/10.1016/S0921-5093(99)00085-4)



131. Lanas J, Alvarez J (2004) Dolomitic limes: evolution of the slaking process under different conditions. *Thermoch Acta* 423:1–12. <https://doi.org/10.1016/j.tca.2004.04.016>
132. Lanas J, Alvarez JI (2004) Dolomitic lime: thermal decomposition of nesquehonite. *Thermochim Acta* 421:123–132. <https://doi.org/10.1016/j.tca.2004.04.007>
133. Moşoiu C, Vlase D, Vlase G et al (2019) TG-DTA and FTIR analyses of roman and later historic mortars from Drobeta-Turmu Severin region. *J Therm Anal Calorim* 138:2159–2166. <https://doi.org/10.1007/s10973-019-08508-x>
134. Cardoso I, Macedo MF, Vermeulen F et al (2014) A multidisciplinary approach to the study of archaeological mortars from the town of Ammaia in the Roman Province of Lusitania (Portugal). *Archaeometry* 56:1–24. <https://doi.org/10.1111/arem.12020>
135. Miriello D, Bloise A, Crisci GM et al (2013) Compositional analysis of mortars from the late antique site of Son Peretó (Mallorca, Balearic Island, Spain): archaeological implications. *Archaeometry* 55:1101–1121. <https://doi.org/10.1111/j.1475-4754.2012.00732.x>
136. Montoya C, Lanas J, Arandigoyen M et al (2003) Study of ancient dolomitic mortars of the church of Santa María de Zamarce in Navarra (Spain): comparison with simulated standards. *Thermoch Acta* 398:107–122. [https://doi.org/10.1016/S0040-6031\(02\)00321-0](https://doi.org/10.1016/S0040-6031(02)00321-0)
137. Unluer C, Al-Tabbaa A (2014) Characterization of light and heavy hydrated magnesium carbonates using thermal analysis. *J Therm Anal Calorim* 115:595–607. <https://doi.org/10.1007/s10973-013-3300-3>
138. Katayama T (2010) The so-called alkali-carbonate reaction (ACR) – its mineralogical and geochemical details, with special reference to ASR. *Cem Concr Res* 40:643–675. <https://doi.org/10.1016/j.cemconres.2009.09.020>
139. Štukovnik P, Marinšek M, Mirtič B, Bokan Bosiljkov V (2015) Influence of alkali carbonate reaction on compressive strength of mortars with air lime binder. *Constr Build Mater* 75:247–254. <https://doi.org/10.1016/j.conbuildmat.2014.11.024>
140. Štukovnik P, Bokan BV, Marinšek M (2020) Alkali-dolomite reaction in air lime mortar—implications for increased strength and water resistance. *J Cult Herit* 45:160–168. <https://doi.org/10.1016/j.culher.2020.02.007>
141. Sabbioni C, Zappia G, Riontino C et al (2001) Atmospheric deterioration of ancient and modern hydraulic mortars. *Atmos Environ* 35:539–548. [https://doi.org/10.1016/S1352-2310\(00\)00310-1](https://doi.org/10.1016/S1352-2310(00)00310-1)
142. Sabbioni C, Bonaza A, Zappia G (2002) Damage on hydraulic mortars: the Venice Arsenal. *J Cult Herit* 3:83–88. [https://doi.org/10.1016/S1296-2074\(02\)01163-9](https://doi.org/10.1016/S1296-2074(02)01163-9)
143. Natural hydraulic limes, Mineral Planning Factsheet, British Geological Survey, Natural Environment Research Council. www.bgs.ac.uk/mineralsUK/planning/mineralPlanningFactsheets.html
144. Rassinoux F, Petit JC, Meunier A (1989) Ancient analogues of modern cement: calcium hydrosilicates in mortars and concretes from Gallo-Roman thermal baths of Western France. *J Am Ceram Soc* 72:1026–1032. <https://doi.org/10.1111/j.1151-2916.1989.tb06263.x>
145. Válek J, van Halem E, Viani A et al (2014) Determination of optimal burning temperature ranges for production of natural hydraulic limes. *Constr Build Mater* 66:771–780. <https://doi.org/10.1016/j.conbuildmat.2014.06.015>
146. Gulotta D, Goidanich S, Tedeschi C et al (2013) Commercial NHL-containing mortars for the preservation of historical architecture. Part 1: Compositional and mechanical characterization. *Constr Build Mater* 38:31–42. <https://doi.org/10.1016/j.conbuildmat.2012.08.029>
147. Callebaut K, Elsen J, Van Balen K et al (2001) Nineteenth century hydraulic restoration mortars in the Saint Michael's Church (Leuven, Belgium): natural hydraulic lime or cement? *Cem Concr Res* 31:397–403. [https://doi.org/10.1016/S0008-8846\(00\)00499-3](https://doi.org/10.1016/S0008-8846(00)00499-3)
148. Varas MJ, Alvarez de Buergo M, Fort R (2005) Natural cement as the precursor of Portland cement: methodology for its identification. *Cem Concr Res* 35:2055–2065. <https://doi.org/10.1016/j.cemconres.2004.10.045>
149. Marques SF, Ribeiro RA, Silva LM et al (2006) Study of rehabilitation mortars: construction of a knowledge correlation matrix. *Cem Concr Res* 36:1894–1902. <https://doi.org/10.1016/j.cemconres.2006.06.005>
150. Frankeová D, Koudelková V (2020) Influence of ageing conditions on the mineralogical micro-character of natural hydraulic lime mortars. *Constr Build Mater* 264:120205. <https://doi.org/10.1016/j.conbuildmat.2020.120205>
151. Taylor HFW (1990) *Cement chemistry*. Academic Press, New York
152. Zhang D, Zhao J, Wang D et al (2018) Comparative study on the properties of three hydraulic lime mortar systems: Natural hydraulic lime mortar, cement-aerial lime-based mortar and slag-aerial lime-based mortar. *Constr Build Mater* 186:42–52. <https://doi.org/10.1016/j.conbuildmat.2018.07.053>
153. Lea FM (1970) *The chemistry of cement and concrete*. Edward Arnold, Glasgow
154. Garijo L, Zhang X, Ruiz G et al (2020) Age effect on the mechanical properties of natural hydraulic and aerial lime mortars. *Constr Build Mater* 236:117573. <https://doi.org/10.1016/j.conbuildmat.2019.117573>
155. Wang KS, Lin KL, Lee TY et al (2004) The hydration characteristics when C₂S is present in MSWI fly ash slag. *Cem Concr Comp* 26:323–330. [https://doi.org/10.1016/S0958-9465\(02\)00144-0](https://doi.org/10.1016/S0958-9465(02)00144-0)
156. Kalagri A, Karatasios I, Kilikoglou V (2014) The effect of aggregate size and type of binder on microstructure and mechanical properties of NHL mortars. *Constr Build Mater* 53:467–474. <https://doi.org/10.1016/j.conbuildmat.2013.11.111>
157. Figueiredo C, Lawrence M, Bal, R (2016) Mechanical properties of standard and commonly formulated NHL mortars used for retrofitting. In: Emmitt S, Adeyeye K (eds). *Integrated design conference ID@50: building our future*
158. Apostolopoulou M, Armaghani DJ, Bakolas A et al (2019) Compressive strength of natural hydraulic lime mortars using soft computing techniques. *Procedia Struct Integrity* 17:914–923. <https://doi.org/10.1016/j.prostr.2019.08.122>
159. ANCADE (2014) *Practical guide to lime mortars*.
160. ASTM C 270-14a (2014) *Standard specification for mortar for unit masonry*
161. Cizer Ö (2009) Competition between carbonation and hydration on the hardening of calcium hydroxide and



- calcium silicate binders. Dissertation, Katholieke Universiteit Leuven
162. Arandigoyen M, Bicer-Simsir B, Alvarez JI et al (2006) Variation of microstructure with carbonation in lime and blended pastes. *Appl Surf Sci* 252:7562–7571. <https://doi.org/10.1016/j.apsusc.2005.09.007>
163. Biggs DT (2005) Mortar as grout for reinforced masonry mortar. RBA project 8379
164. Biggs DT (2005) Grouting masonry using portland cement-lime mortars. In: NLA Building Lime Group (eds) International building lime symposium, pp 1–16
165. Bullard JW, Jennings HM, Livingston RA et al (2011) Mechanisms of cement hydration. *Cem Concr Res* 41:1208–1223. <https://doi.org/10.1016/j.cemconres.2010.09.011>
166. Richardson IG (2000) The nature of the hydration products in hardened cement pastes. *Cem Concr Compos* 22:97–113. [https://doi.org/10.1016/S0958-9465\(99\)00036-0](https://doi.org/10.1016/S0958-9465(99)00036-0)
167. Lothenbach B, Nonat A (2015) Calcium silicate hydrates: Solid and liquid phase composition. *Cem Concr Res* 78:57–70. <https://doi.org/10.1016/j.cemconres.2015.03.019>
168. Richardson IG (2008) The calcium silicate hydrates. *Cem Concr Res* 38:137–158. <https://doi.org/10.1016/j.cemconres.2007.11.005>
169. Gallucci E, Scrivener K (2007) Crystallisation of calcium hydroxide in early age model and ordinary cementitious systems. *Cem Concr Res* 37:492–501. <https://doi.org/10.1016/j.cemconres.2007.01.001>
170. Galmarini S, Aimable A, Ruffray N et al (2011) Changes in portlandite morphology with solvent composition: atomistic simulations and experiment. *Cem Concr Res* 41:1330–1338. <https://doi.org/10.1016/j.cemconres.2011.04.009>
171. Hayri U, Baradan B (2011) The effect of curing temperature and relative humidity on the strength development of Portland cement mortar. *Sci Res Essays* 6:2504–2511. <https://doi.org/10.5897/SRE11.269>
172. Lothenbach B, Winnefeld F, Alder C et al (2007) Effect of temperature on the pore solution, microstructure and hydration products of Portland cement pastes. *Cem Concr Res* 37:483–491. <https://doi.org/10.1016/j.cemconres.2006.11.016>
173. Gallucci E, Zhang X, Scrivener KL (2013) Effect of temperature on the microstructure of calcium silicate hydrate (C–S–H). *Cem Concr Res* 53:185–195. <https://doi.org/10.1016/j.cemconres.2013.06.008>
174. Lothenbach B, Winnefeld F (2006) Thermodynamic modelling of the hydration of Portland cement. *Cem Concr Res* 36:209–226. <https://doi.org/10.1016/j.cemconres.2005.03.001>
175. Bahafid S, Ghabezloo S, Duc M et al (2017) Effect of the hydration temperature on the microstructure of Class G cement: C–S–H composition and density. *Cem Concr Res* 95:270–328. <https://doi.org/10.1016/j.cemconres.2017.02.008>
176. Ramachandran VS, Paroli RM, Beaudoin JJ, Delgado AH (2003) Handbook of thermal analysis of construction materials
177. Bonavetti V, Rahhal V, Irassar I (2001) Studies on the carboaluminate formation in limestone filler-blended cements. *Cem Concr Res* 31:853–859. [https://doi.org/10.1016/S0008-8846\(01\)00491-4](https://doi.org/10.1016/S0008-8846(01)00491-4)
178. Matschei T, Lothenbach B, Glasser FP (2007) The role of calcium carbonate in cement hydration. *Cem Concr Res* 37:551–558. <https://doi.org/10.1016/j.cemconres.2006.10.013>
179. Gartner EM, Young JF, Damidot D, Jawed I (2001) Hydration of portland cement. In: Bensted J, Barnes P (eds) Structure and performance of cements, 2nd edn. CRC Press, Florida, pp 1–19
180. Ipavec A, Gabrovšek R, Vuk T et al (2011) Carboaluminate phases formation during the hydration of calcite-containing portland cement. *J Am Ceram Soc* 94:1238–1242. <https://doi.org/10.1111/j.1551-2916.2010.04201.x>
181. Gopi S, Subramanian VK, Palanisamy K (2013) Aragonite-calcite-vaterite: a temperature influenced sequential polymorphic transformation of CaCO₃ in the presence of DTPA. *Mater Res Bull* 48:1906–1912. <https://doi.org/10.1016/j.materresbull.2013.01.048>
182. Cizer Ö, Rodriguez-Navarro C, Ruiz-Agudo E et al (2012) Phase and morphology evolution of calcium carbonate precipitated by carbonation of hydrated lime. *J Mater Sci* 47:6151–6165. <https://doi.org/10.1007/s10853-012-6535-7>
183. Jung WM, Kang SH, Kim WS et al (2000) Particle morphology of calcium carbonate precipitated by gas-liquid reaction in a Couette-Taylor reactor. *Chem Eng Sci* 55:733–747. [https://doi.org/10.1016/S0009-2509\(99\)00395-4](https://doi.org/10.1016/S0009-2509(99)00395-4)
184. Cizer O, Van Balen K, Elsen J, Van Gemert D (2008) Crystal morphology of precipitated calcite crystals from accelerated carbonation of lime binders. In: Baccocchi R, Costa G, Poletti A, Pomi R (eds) Conference on accelerated carbonation for environmental and materials engineering, pp 149–158
185. Groves GW, Rodway DI, Richardson IG (1990) The carbonation of hardened cement pastes. *Adv Cem Res* 3:117–125. <https://doi.org/10.1680/adcr.1990.3.11.117>
186. Black L, Garbev K, Gee I (2008) Surface carbonation of synthetic C–S–H samples: A comparison between fresh and aged C–S–H using X-ray photoelectron spectroscopy. *Cem Concr Res* 38:745–750. <https://doi.org/10.1016/j.cemconres.2008.02.003>
187. Chen JJ, Thomas JJ, Jennings HM (2006) Decalcification shrinkage of cement paste. *Cem Concr Res* 36:801–809. <https://doi.org/10.1016/j.cemconres.2005.11.003>
188. Chen JJ, Thomas JJ, Jennings HM (2015) Preparation of single-phase C–S–H specimens from hydrated tricalcium silicate pastes. <https://doi.org/10.13140/RG.2.1.4017.0401>
189. Hendrickx R (2009) The adequate measurement of the workability of masonry mortar. Ph.D. dissertation, Katholieke Universiteit Leuven
190. Fourmentin M, Faure P, Gauffinet S et al (2015) Porous structure and mechanical strength of cement-lime pastes during setting. *Cem Concr Res* 77:1–8. <https://doi.org/10.1016/j.cemconres.2015.06.009>



191. Walker R, Pavia S (2011) Physical properties and reactivity of pozzolans, and their influence on the properties of lime–pozzolan pastes. *Mater Struct* 44:1139–1150. <https://doi.org/10.1617/s11527-010-9689-2>
192. Tironi A, Trezza MA, Scian AN et al (2013) Assessment of pozzolanic activity of different calcined clays. *Cem Concr Comp* 37:319–327. <https://doi.org/10.1016/j.cemconcomp.2013.01.002>
193. Charola AE, Faria Rodrigues P, McGhie AR et al (2005) Pozzolanic components in lime mortars: correlating behaviour, composition and microstructure. *Restor Build Monum* 11:111–118. <https://doi.org/10.1515/rbm-2005-5942>
194. Ilić BR, Mitrović AA, Miličić L (2010) Thermal treatment of kaolin clay to obtain metakaolin. *RHemijska industrija* 64:351–356. <https://doi.org/10.2298/HEMIND100322014>
195. Baronio G, Binda L (1997) Study of the pozzolanicity of some bricks and clays. *Constr Build Mater* 11:41–46. [https://doi.org/10.1016/S0950-0618\(96\)00032-3](https://doi.org/10.1016/S0950-0618(96)00032-3)
196. Mohammed S (2017) Processing, effect and reactivity assessment of artificial pozzolans obtained from clays and clay wastes: a review. *Constr Build Mater* 140:10–19. <https://doi.org/10.1016/j.conbuildmat.2017.02.078>
197. Zhou YF, Li JS, Lu JX et al (2020) Sewage sludge ash: a comparative evaluation with fly ash for potential use as lime–pozzolan binders. *Constr Build Mater* 242:118160. <https://doi.org/10.1016/j.conbuildmat.2020.118160>
198. Almeida J, SantosSilva A, Faria P, Ribeiro A (2020) Assessment on tungsten mining residues potential as partial cement replacement. *KnE Eng* 5:228–237. <https://doi.org/10.18502/keg.v5i4.6814>
199. Navrátilová E, Rovnaníková P (2016) Pozzolanic properties of brick powders and their effect on the properties of modified lime mortars. *Constr Build Mater* 120:530–539. <https://doi.org/10.1016/j.conbuildmat.2016.05.062>
200. Cerný R, Kunca A, Tydlitá V et al (2006) Effect of pozzolanic admixtures on mechanical, thermal and hygric properties of lime plasters. *Constr Build Mater* 20:849–857. <https://doi.org/10.1016/j.conbuildmat.2005.07.002>
201. Faria P (2009) Resistance to salts of lime and pozzolan mortars. In: Groot C (ed) *International RILEM workshop on repair mortars for historic masonry*, pp 99–110
202. Donatello S, Tyrer M, Cheeseman CR (2010) Comparison of test methods to assess pozzolanic activity. *Cem Concr Comp* 32:121–127. <https://doi.org/10.1016/j.cemconcomp.2009.10.008>
203. Pontes J, Santos Silva A, Faria P (2013) Evaluation of pozzolanic reactivity of artificial pozzolans. *Mater Sci Forum* 730–732:433–438. <https://doi.org/10.4028/www.scientific.net/MSF.730-732.433>
204. AFNOR (2010) NF P 18-513—Métakaolin, addition pouzzolanique pour bétons—Définitions, spécifications, critères de conformité
205. ASTM C593-19 (2019) Standard specification for fly ash and other pozzolans for use with lime for soil stabilization. ASTM International, West Conshohocken. www.astm.org
206. Stefanidou M, Tсадaka EC, Pavlidou E (2017) Influence of nano-silica and nano-alumina in lime–pozzolan and lime–metakaolin binders. *Mater Today: Proceedings* 4:6908–6922. <https://doi.org/10.1016/j.matpr.2017.07.020>
207. Fernández JM, Duran A, Navarro-Blasco I et al (2013) Influence of nanosilica and a polycarboxylate ether superplasticizer on the performance of lime mortars. *Cem Concr Res* 43:12–24. <https://doi.org/10.1016/j.cemconres.2012.10.007>
208. Papayianni I, Pachta V, Stefanidou M (2013) Analysis of ancient mortars and design of compatible repair mortars: the case study of Odeion of the archaeological site of Dion. *Constr Build Mater* 40:84–92. <https://doi.org/10.1016/j.conbuildmat.2012.09.086>
209. Arizzi A, Cultrone G (2018) Comparing the pozzolanic activity of aerial lime mortars made with metakaolin and fluid catalytic cracking catalyst residue: a petrographic and physical-mechanical study. *Constr Build Mater* 184:382–390. <https://doi.org/10.1016/j.conbuildmat.2018.07.002>
210. Grist ER, Paine KA, Heath A et al (2013) Compressive strength development of binary and ternary lime–pozzolan mortars. *Mater Des* 52:514–523. <https://doi.org/10.1016/j.matdes.2013.05.006>
211. Fusade L, Viles H, Wood C et al (2019) The effect of wood ash on the properties and durability of lime mortar for repointing damp historic buildings. *Constr Build Mater* 212:500–513. <https://doi.org/10.1016/j.conbuildmat.2019.03.326>
212. Veiga R, Velosa A, Magalhães A (2009) Experimental applications of mortars with pozzolanic additions: characterization and performance evaluation. *Constr Build Mater* 23:318–327. <https://doi.org/10.1016/j.conbuildmat.2007.12.003>
213. Torres I, Matias G, Faria P (2020) Natural hydraulic lime mortars—the effect of ceramic residues on physical and mechanical behavior. *J Build Eng* 32:101747. <https://doi.org/10.1016/j.job.2020.101747>
214. Oliveira Mateus A, Azenha M, Lourenço PB et al (2017) Experimental analysis of the carbonation and humidity diffusion processes in aerial lime mortar. *Constr Build Mater* 148:38–48. <https://doi.org/10.1016/j.conbuildmat.2017.04.120>
215. Seabra MP, Paiva H, Labrincha JA et al (2009) Admixtures effect on fresh state properties of aerial lime based Mortars. *Constr Build Mater* 23:1147–1153. <https://doi.org/10.1016/j.conbuildmat.2008.06.008>
216. Arizzi A, Cultrone G (2013) The influence of aggregate texture, morphology and grading on the carbonation of non-hydraulic (aerial) lime-based mortars. *Q J Eng Geol Hydrogeol* 46:507–520. <https://doi.org/10.1144/qjegh2012-017>
217. Lanás J, Sirera R, Alvarez JI (2005) Compositional changes in lime-based mortars exposed to different environments. *Thermochim Acta* 429:219–226. <https://doi.org/10.1016/j.tca.2005.03.015>
218. Boynton RS (1984) Lime and limestone in encyclopedia of chemical technology. Wiley, New York
219. Balksten K, Klasén K (2005) The Influence of craftsmanship on the inner structures of lime plasters. In: Balksten (ed) *International RILEM workshop repair mortars for historic masonry*, vol 1, pp 11–20

220. Cizer Ö, Van Balen K, Van Gemert D (2010) Competition between hydration and carbonation in hydraulic lime and lime-Pozzolana Mortars. *Adv Mater Res* 133–134:241–246. <https://doi.org/10.4028/www.scientific.net/AMR.133-134.241>
221. Bakolas A, Aggelakopoulou E, Moropoulou A et al (2006) Evaluation of pozzolanic activity and physicochemical characteristics in metakaolin-lime pastes. *J Therm Anal Calorim* 84:157–163. <https://doi.org/10.1007/s10973-005-7262-y>
222. Cabrera J, Frías M (2001) Influence of MK on the reaction kinetics in MK/lime and MK-blended cement systems at 20°C. *Cem Concr Res* 31:519–527. [https://doi.org/10.1016/S0008-8846\(00\)00465-8](https://doi.org/10.1016/S0008-8846(00)00465-8)
223. Aggelakopoulou E, Bakolas A, Moropoulou A (2011) Properties of lime–metakolin mortars for the restoration of historic masonries. *Appl Clay Sci* 53:15–19. <https://doi.org/10.1016/j.clay.2011.04.005>
224. Kapetanaki K, Kapridaki C, Maravelaki PN (2019) Nano-TiO₂ in hydraulic lime-metakaolin mortars for restoration projects: physicochemical and mechanical assessment. *Buildings* 9:236. <https://doi.org/10.3390/buildings9110236>
225. Zhang D, Zhao J, Wang D et al (2020) Influence of pozzolanic materials on the properties of natural hydraulic lime based mortars. *Constr Build Mater* 244:118360. <https://doi.org/10.1016/j.conbuildmat.2020.118360>

Publisher's Note Springer Nature remains neutral with regard to jurisdictional claims in published maps and institutional affiliations.

